

Advanced Model Development for Large Eddy Simulation of Oxy-Combustion and Supercritical CO₂ Power Cycles

**Joe Oefelein, Adam Steinberg, Devesh Ranjan,
Dhruv Purushotham, Chang Hyeon Lim,
Vedanth Nair, Chris Balance, Stephen Johnston**

**Daniel Guggenheim School of Aerospace Engineering
George W. Woodruff School of Mechanical Engineering
Georgia Institute of Technology, Atlanta, GA 30332**

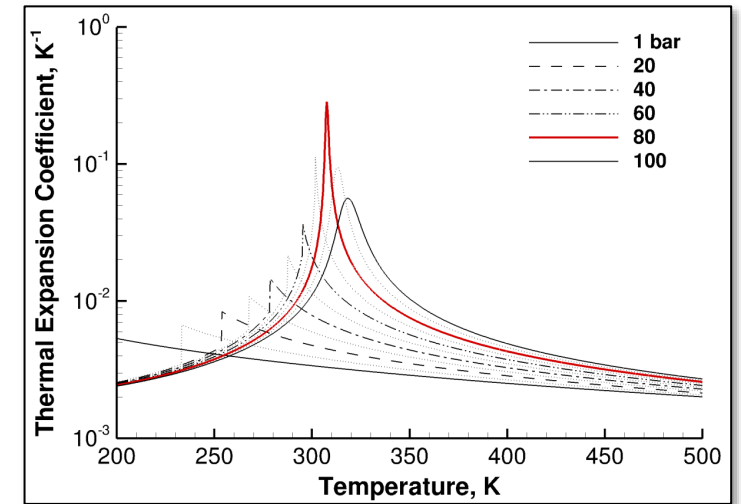
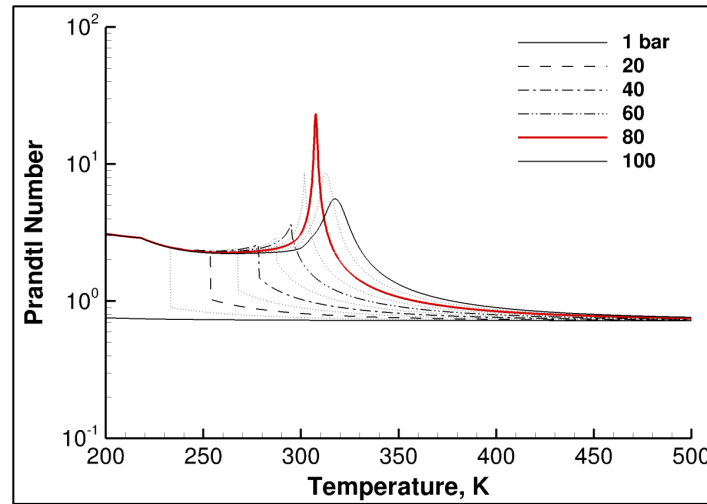
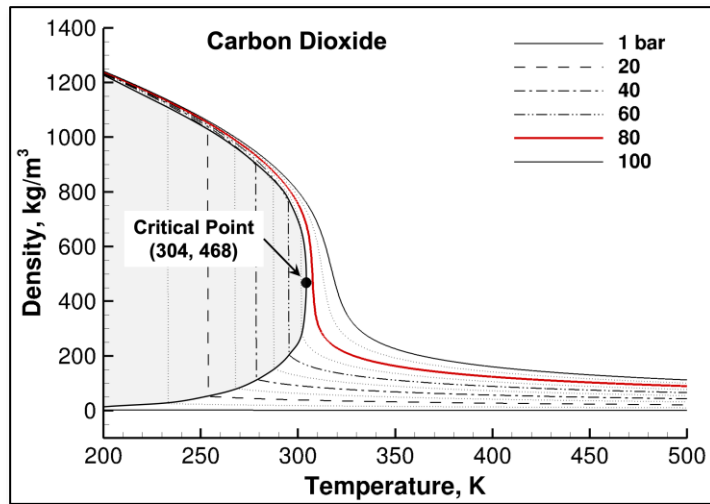
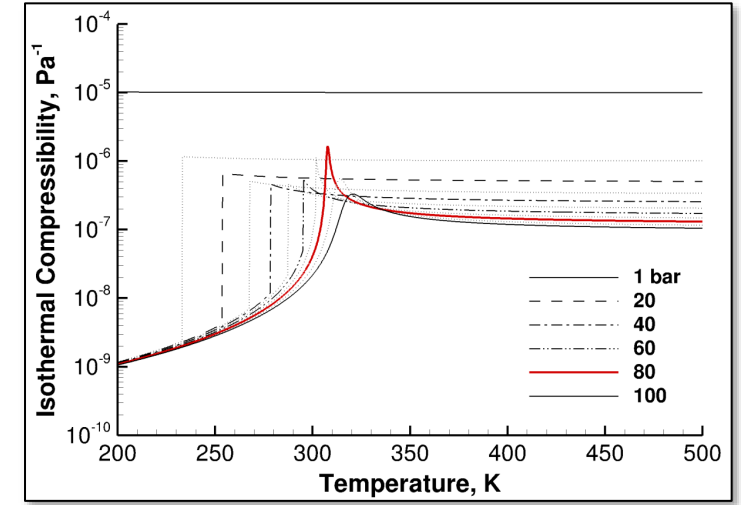
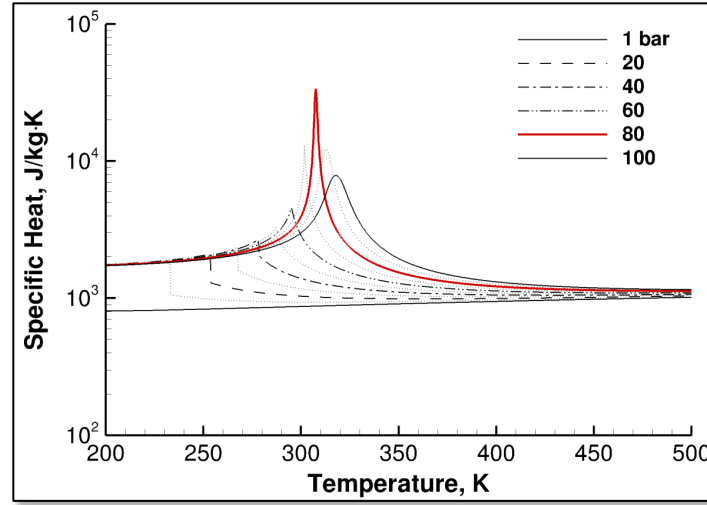
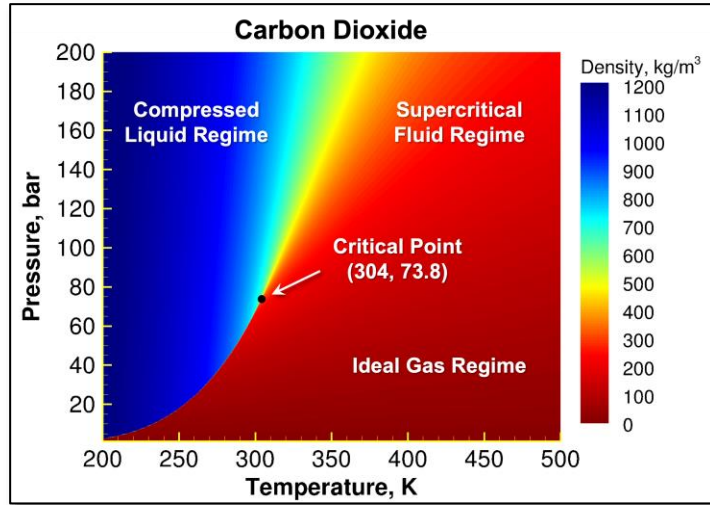
Brian Connolly, Nathan Andrews, Steve White

**Propulsion and Energy Machinery Technologies
Southwest Research Institute, San Antonio, TX 78238**

Project objective

- **Development and validation of predictive models for treatment of direct sCO₂ power cycles through a synergistic combination of computational and experimental research**
 - **Multiphysics model development using DNS/LES (Oefelein/Connolly/Andrews)**
 - Detailed treatment of high-pressure (supercritical) flow processes inherent to oxy-fueled combustion
 - Progression from canonical laboratory-scale studies to device-scale conditions and geometries (e.g., 1500 K, 30 MPa turbine inlet conditions)
 - **Experiments for model validation using a combination of laser and optical measurement techniques (Steinberg/Ranjan/White)**
 - Mixing layer dynamics in sCO₂ loop at Georgia Tech (i.e., Density measurements using 2D burst-mode Raman scattering)
 - 1 MW sCO₂ combustor at Southwest Research Institute (i.e., Chemiluminescence imaging of H₂O and post-flame CO₂)

Supercritical fluids pose unique additional modeling challenges due to highly nonlinear property variations



- **Task 1.0: Project Management and Planning**
- **Task 2.0: Multiphysics Model Development**
 - Subtask 2.1: Unit physics model evaluation and verification studies
 - Subtask 2.2: Treatment of turbulent multiscale mixing processes
 - Subtask 2.3: Treatment of turbulence-chemistry interactions
- **Task 3.0: Benchmark Large Eddy Simulations**
 - Subtask 3.1: Model validation (Georgia Tech sCO₂ Loop)
 - Subtask 3.2: Model validation (SwRI 1 MW Oxy-Fueled sCO₂ Combustor)
 - Subtask 3.3: Parametric Analysis
- **Task 4.0: Experiments for Model Validation**
 - Subtask 4.1: Non-reacting density and velocity measurements in redesigned test section
 - Subtask 4.2: Preliminary IR measurements in 1 MW oxy-fueled sCO₂ combustor
 - Subtask 4.3: Complete IR measurements in 1 MW oxy-fueled sCO₂ combustor

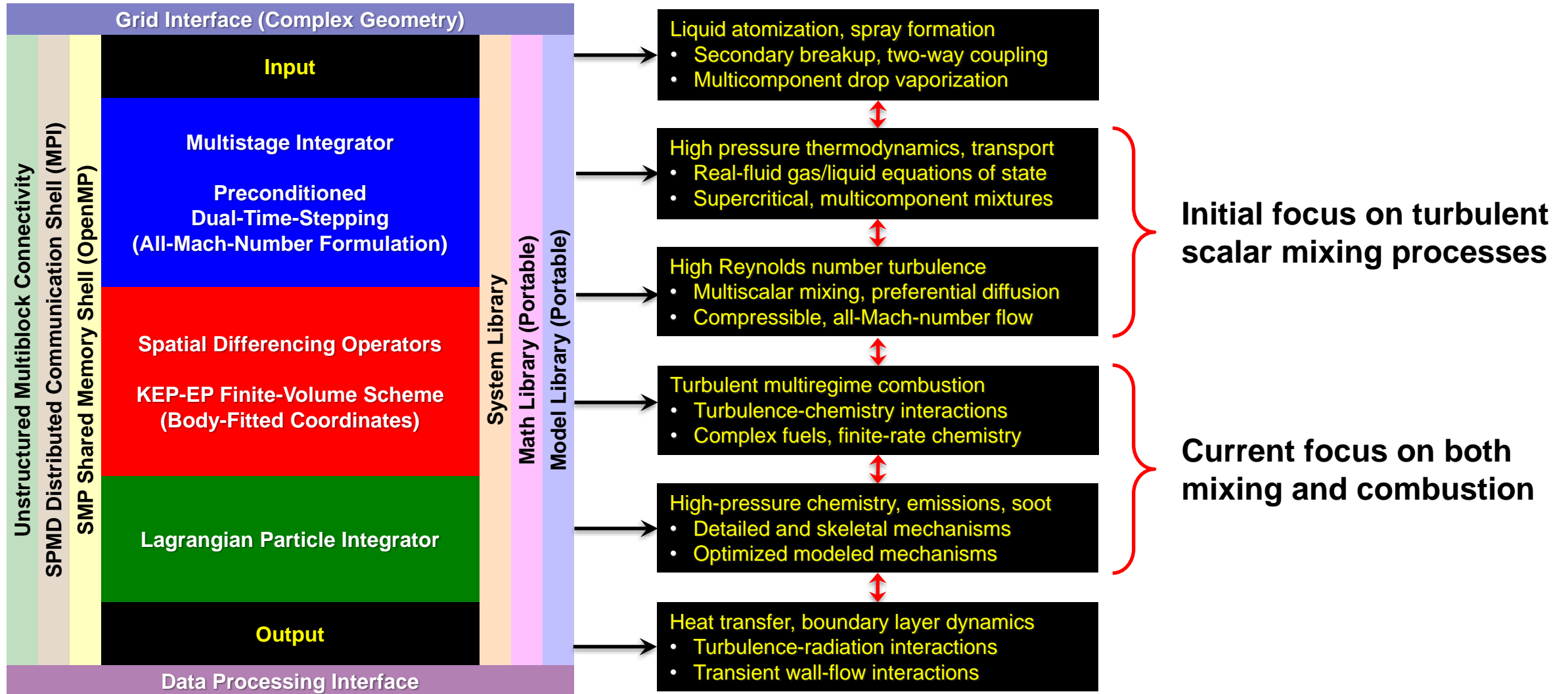
Detailed analysis and model development enabled using RAPTOR code suite designed for DNS/LES

- **Theoretical framework (Comprehensive)**
 - Fully-coupled, compressible conservation equations
 - Nonideal gas/liquid equation of state (high-pressure phenomena)
 - Detailed thermodynamics, transport with finite-rate chemistry
 - Multiphase flow with interface tracking (LS-GFM), spray (Lagrangian-Eulerian)
 - Dynamic subfilter modeling (no tuned constants)
 - Fully-integrated CHT and FSI (in progress)
- **Numerical framework (High-quality)**
 - Kinetic-energy/entropy preserving (non-dissipative, discretely conservative)
 - All-Mach-number (dual-time stepping with generalized preconditioning)
 - Complex geometry and BC's
- **Massively-parallel (Highly-scalable)**



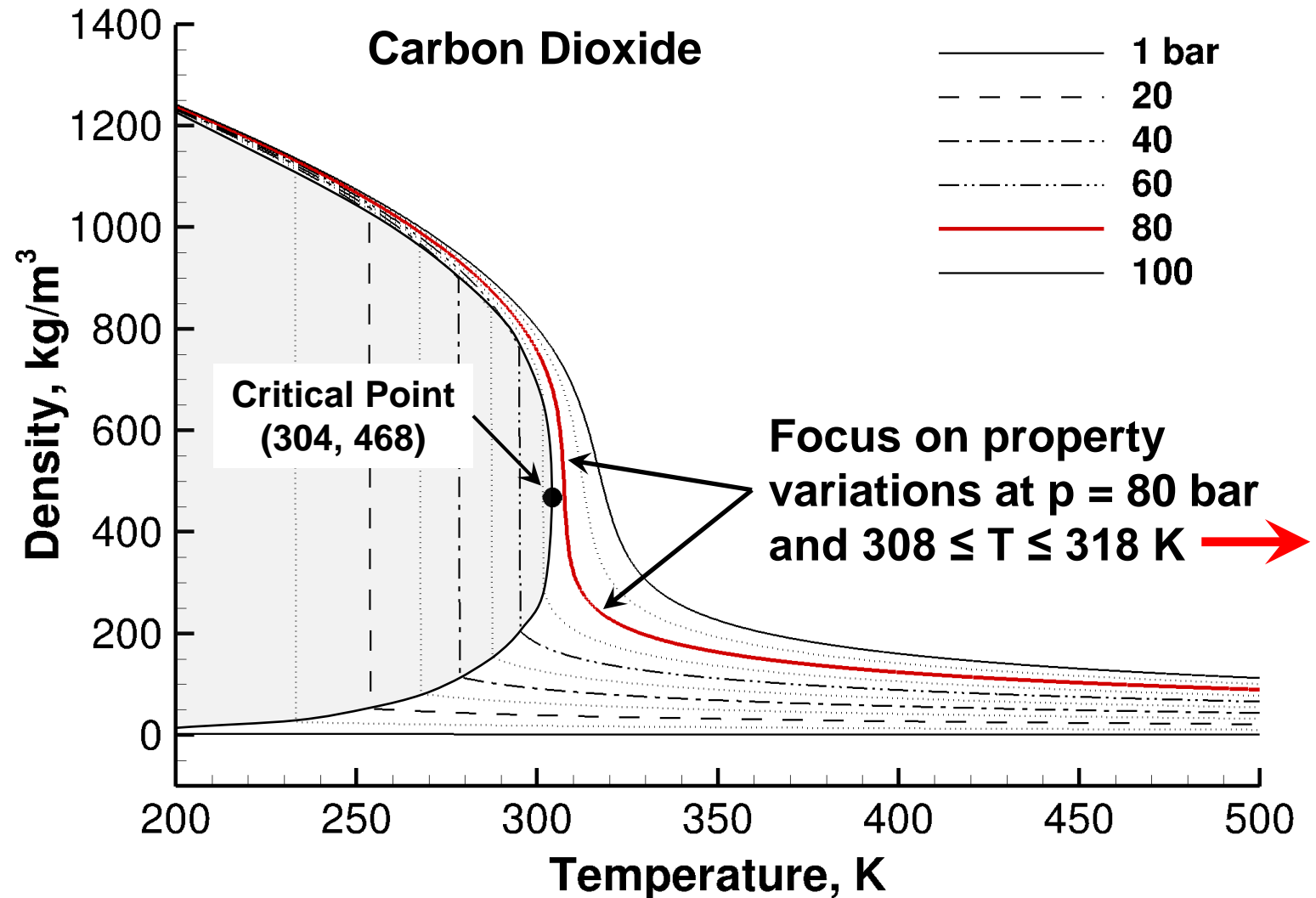
Project selected to receive 2020-2021 ASCR Leadership Computing Challenge (ALCC) award

Detailed analysis and model development enabled using RAPTOR code suite designed for DNS/LES

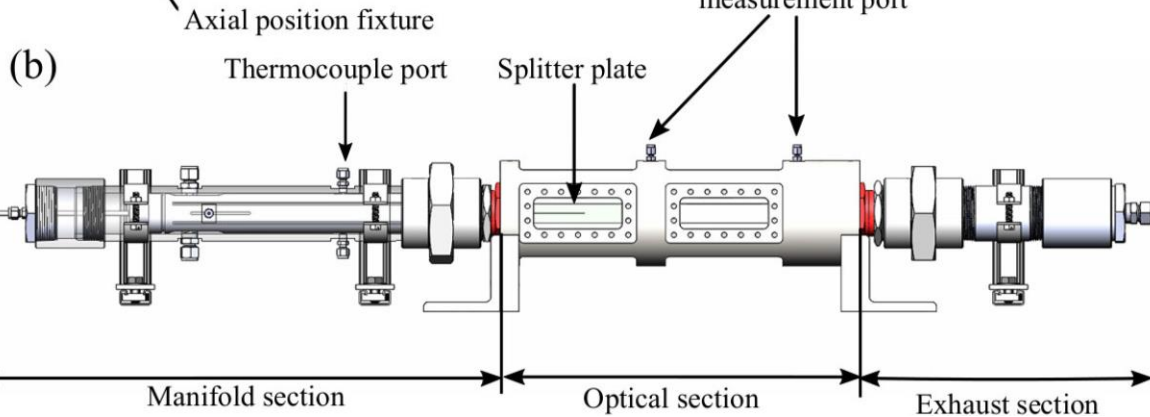
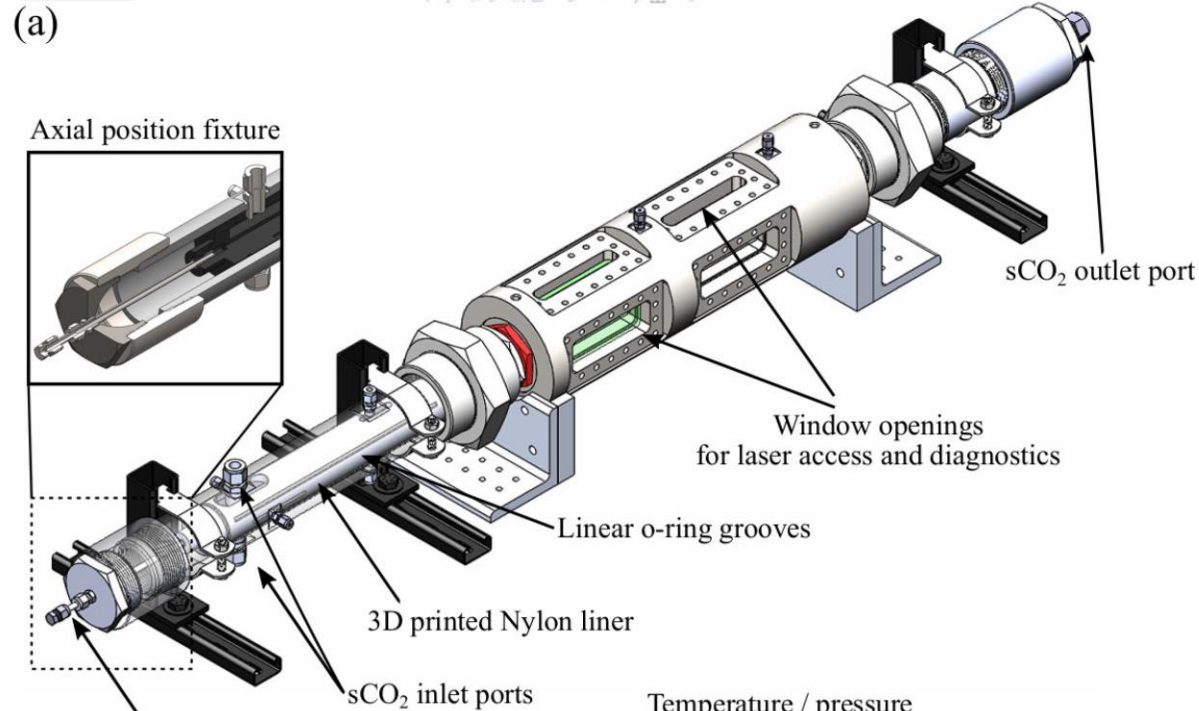


Simulations performed using completely general treatment EOS, thermodynamic, and transport properties

- **State-of-the-art formulation for EOS, thermodynamics, transport, and interfacial properties based on NIST expertise over decades**
 - Real-fluid mixture properties obtained using Extended Corresponding States model
 - Multicomponent formulation using Cubic (e.g., SRK, PR), BWR, or Helmholtz EOS
 - Generalized to treat wide range of hydrocarbon mixtures (Fuel/Oxidizer/Products)
- Custom stand-alone software designed to run efficiently on HPC platforms

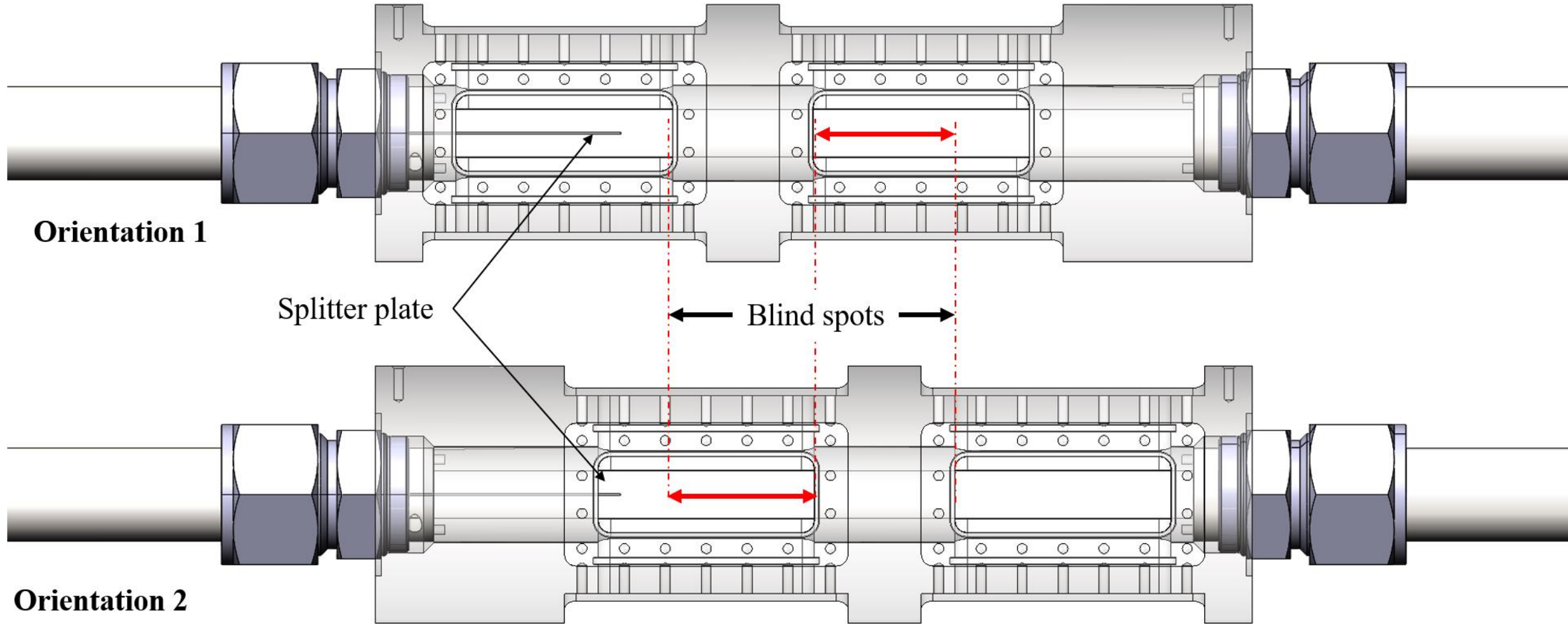


Georgia Tech sCO₂ loop designed to provide insights into supercritical fluid mixing (80 bar, 308 ≤ T ≤ 318 K)

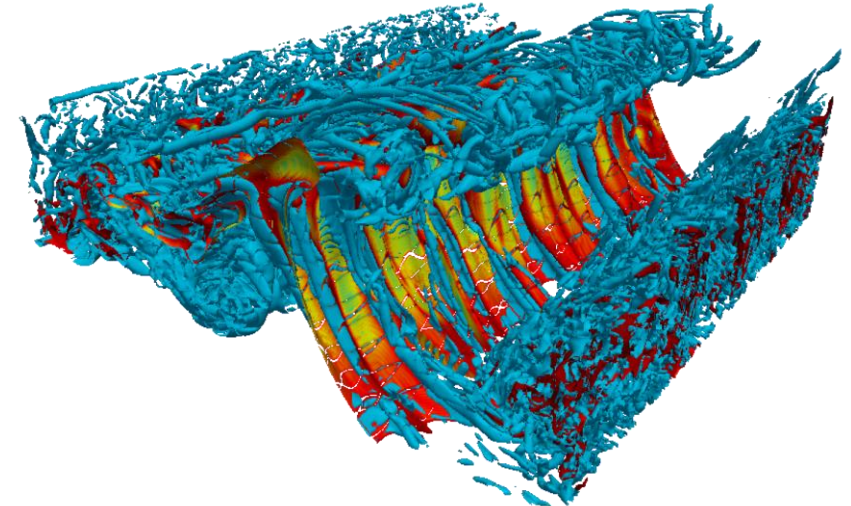
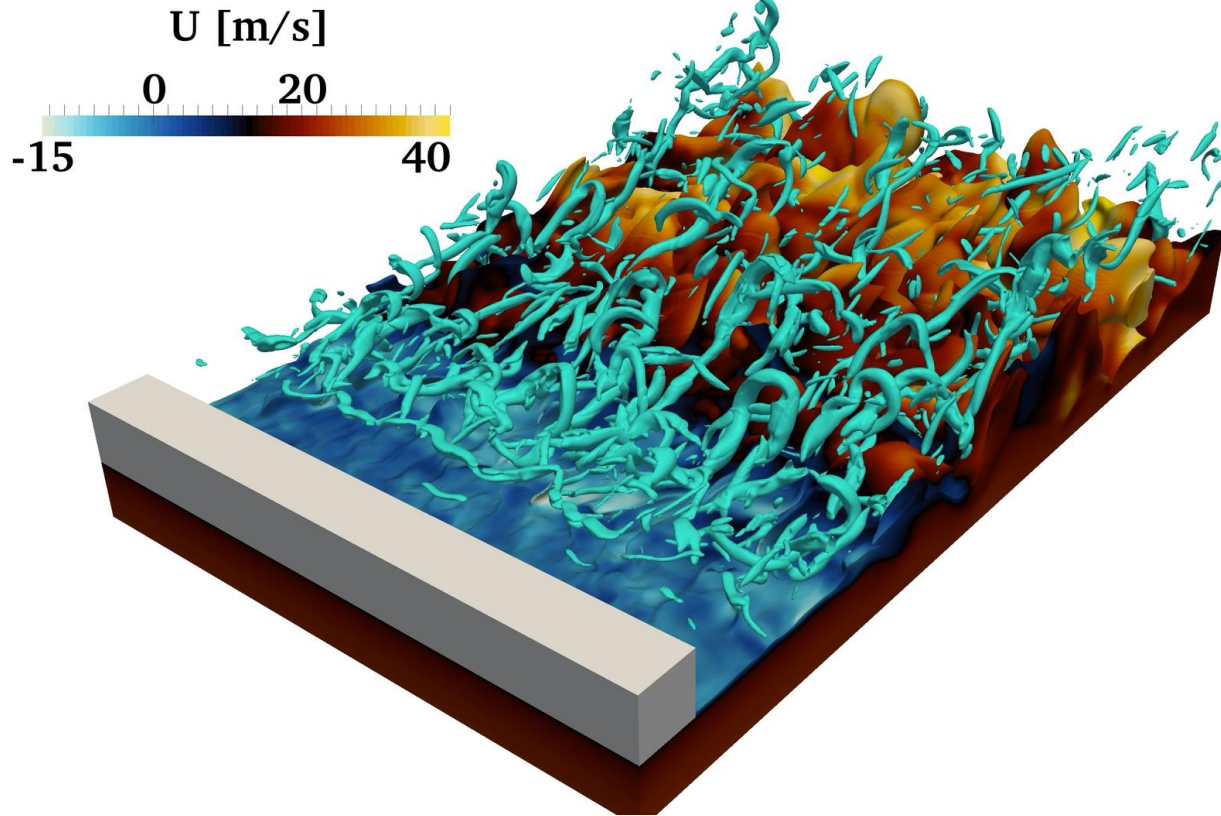


	Pressure [MPa / psi]	Temperature [K / F]	Re	Density [kg/m ³]	Velocity [m/s]
Upper Stream	8 / 1160	308 / 94.7	1.26e5	419.08	0.55
Lower Stream	8 / 1160	318 / 113	4.48e4	241.04	0.11

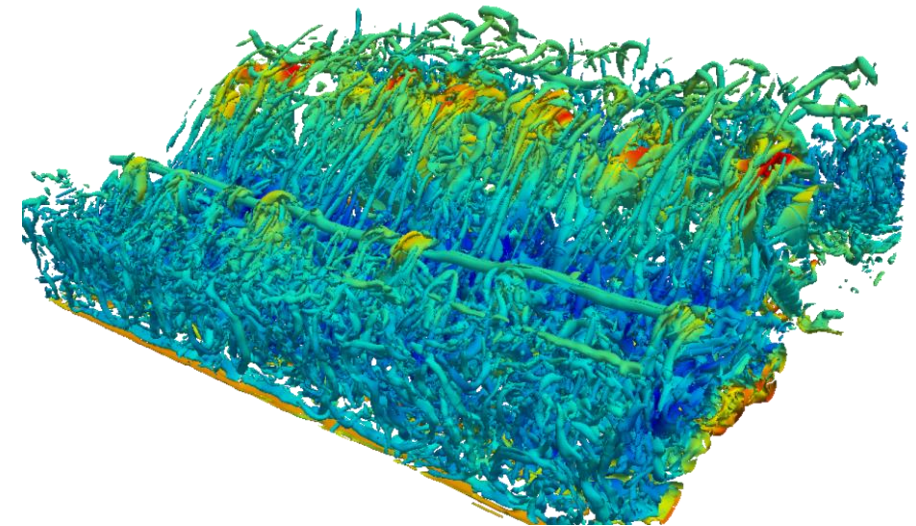
Test section is designed to give full optical access across the entire axial span of the mixing layer



Detailed analysis supported via progression of 2D/3D DNS and LES



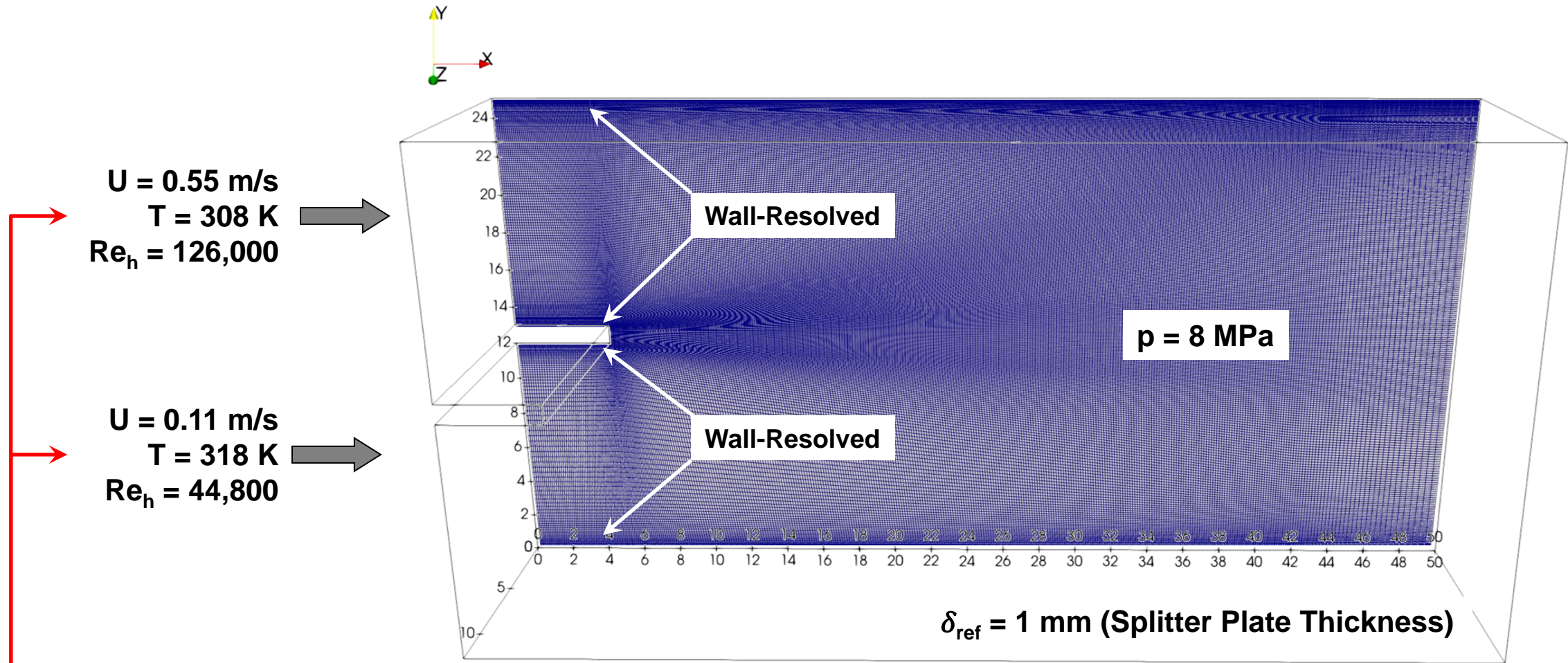
Vorticity and Mixture Fraction



Scalar-Dissipation Field

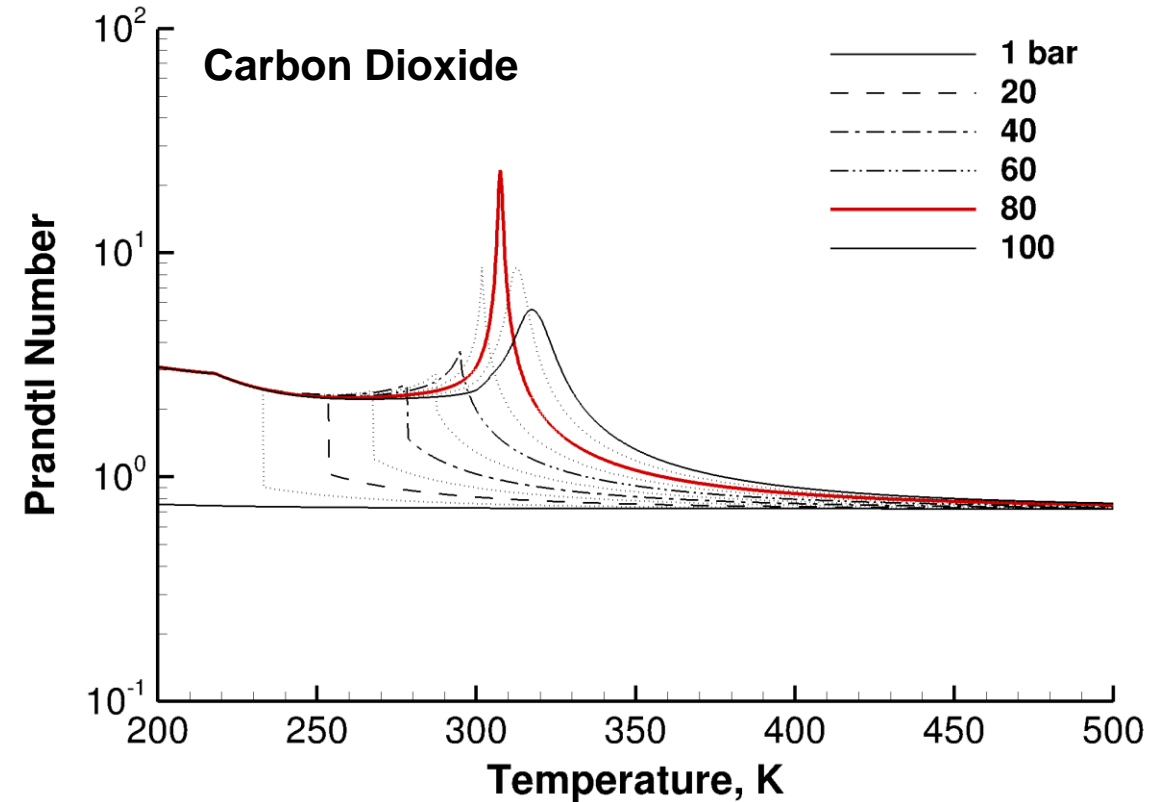
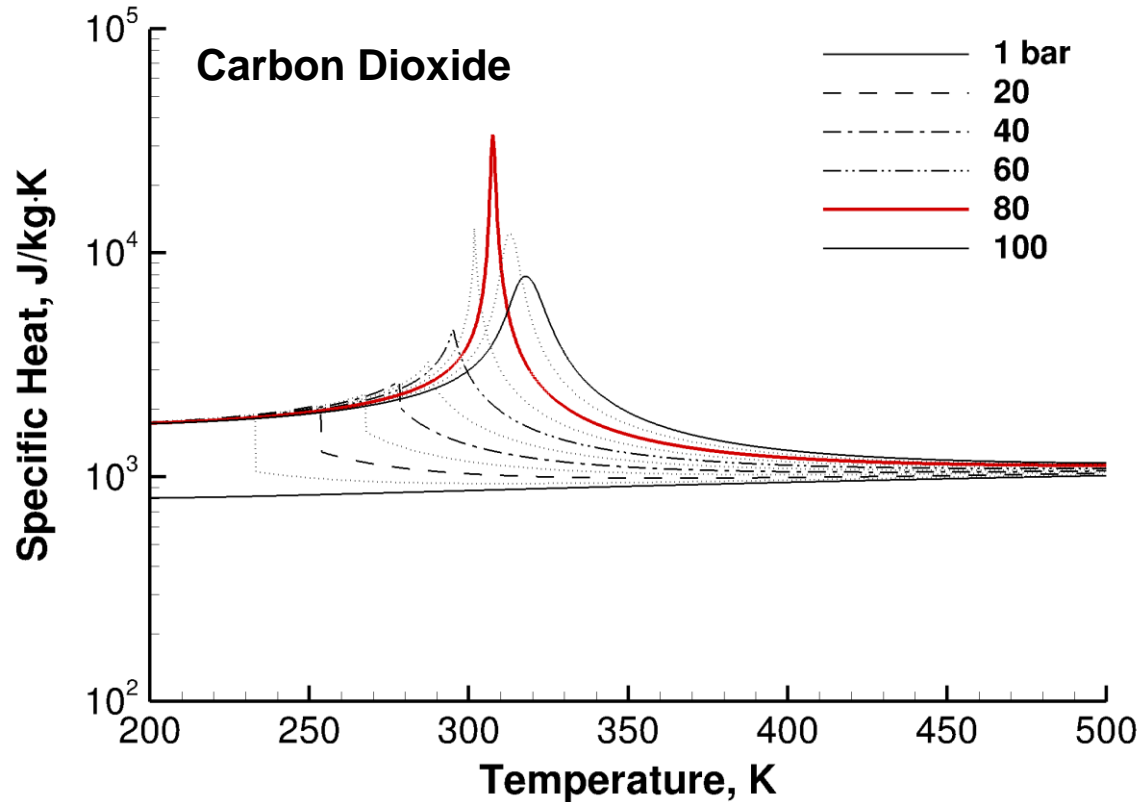
Goal: Facilitate analysis required to understand basic physics and model injection/mixing/combustion processes unique to high-pressure (supercritical) power and propulsion systems

Computational domain and grid match experiment (WRLES completed, full DNS in progress)



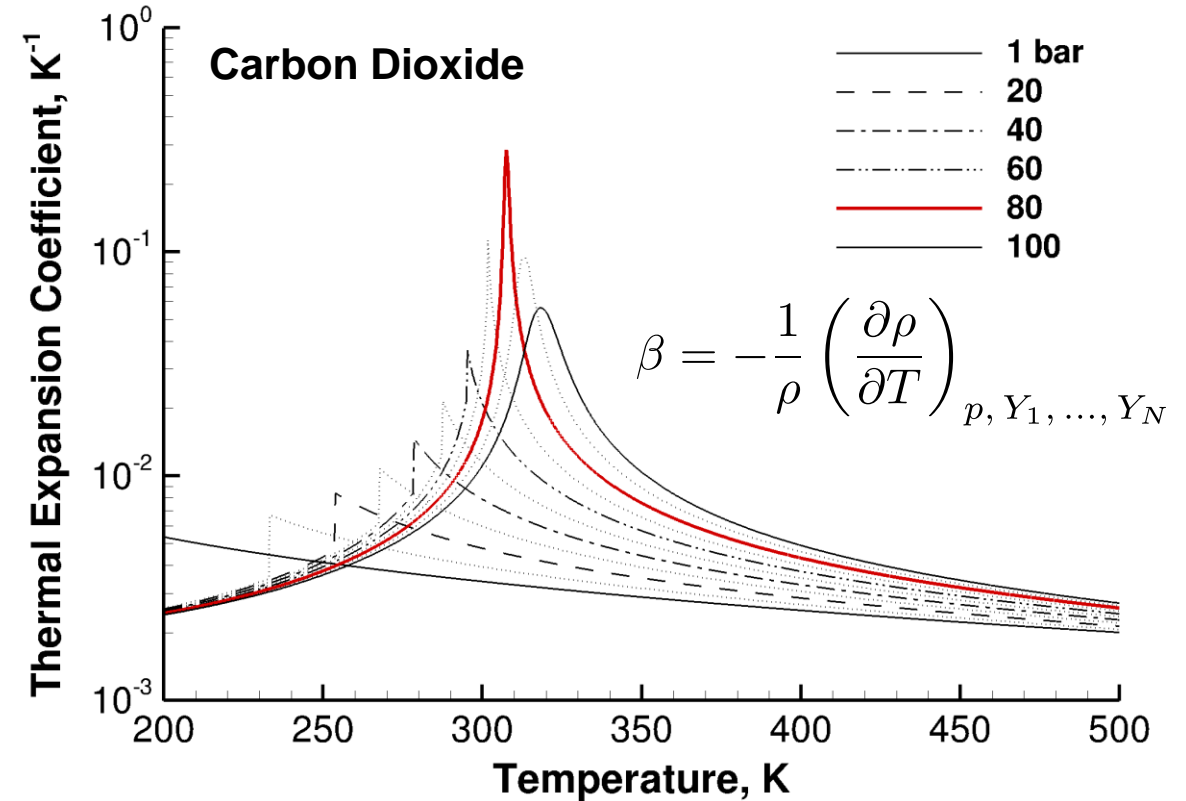
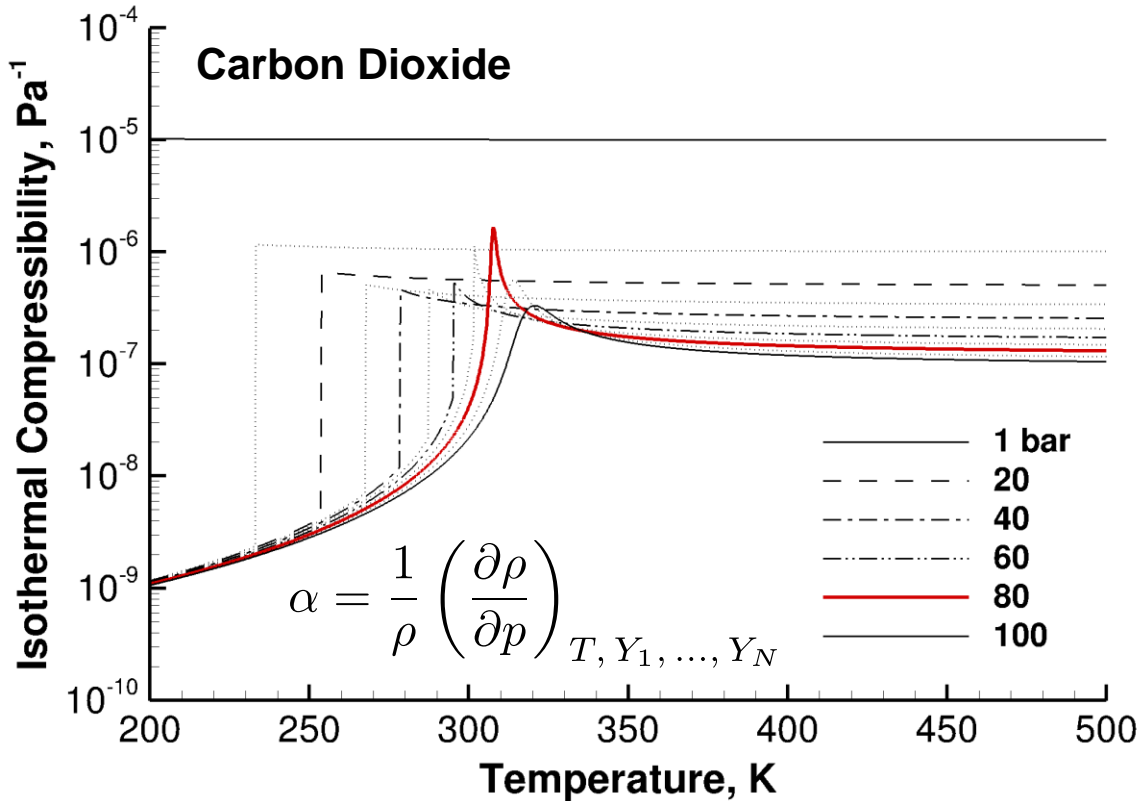
Time-dependent turbulent inflow fluctuations imposed using Synthetic Eddy Method

How do nonlinear property variations affect flow and what are the implications with respect to modeling?



- Heat capacity of the fluid increases dramatically (e.g., more than an order of magnitude between 1 bar and 80 bar over the interval $308 \leq T \leq 318$ K)
- Similarly, significant increases in the Prandtl number are induced (e.g., more than an order of magnitude between 1 bar and 80 bar over the interval $308 \leq T \leq 318$ K)

How do nonlinear property variations affect flow and what are the implications with respect to modeling?



- Two forms of compressibility must be considered
 - Isothermal compressibility ... change in volume due to change in pressure at constant temperature
 - Coefficient of thermal expansion ... change in volume due to change in temperature at constant pressure

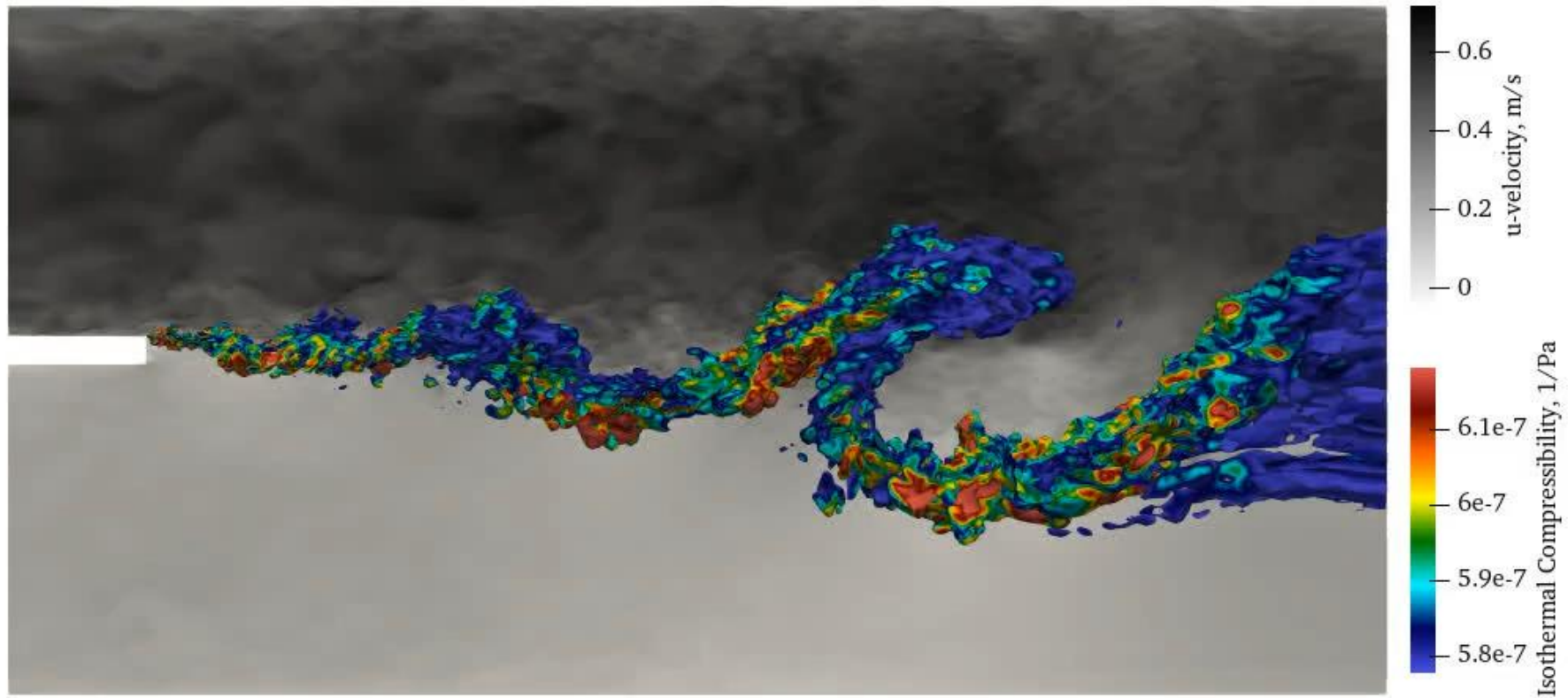
Rate of change in pressure and temperature can be significantly modulated by these nonlinearities

$$\begin{aligned}
 \frac{\partial p}{\partial t} = & -\frac{c^2}{\rho C_p} \left\{ \left[\rho_T h + \rho C_p - \sum_{i=1}^{N-1} (\rho_T h_{Y_i} - \rho_{Y_i} C_p) Y_i \right] \underbrace{\nabla \cdot (\rho \mathbf{u})}_{\text{Mass}} \right. \\
 & + \rho_T \left(\underbrace{\mathbf{u} \cdot \nabla p + M^2 \tau : \nabla \mathbf{u}}_{\text{Momentum}} - \underbrace{\nabla \cdot (\rho h \mathbf{u}) + \nabla \cdot \mathbf{q}_e}_{\text{Total Energy}} \right) \\
 & \left. + \sum_{i=1}^{N-1} (\rho_T h_{Y_i} - \rho_{Y_i} C_p) \left(\underbrace{\nabla \cdot (\rho Y_i \mathbf{u}) - \nabla \cdot \mathbf{q}_i - \dot{\omega}_i}_{\text{Species}} \right) \right\} \\
 \frac{\partial T}{\partial t} = & \frac{c^2}{\rho C_p} \left\{ \left[\rho_p h + \rho_T \frac{T}{\rho} - \sum_{i=1}^{N-1} \left(\rho_p h_{Y_i} - \rho_{Y_i} \rho_T \frac{T}{\rho^2} \right) Y_i \right] \underbrace{\nabla \cdot (\rho \mathbf{u})}_{\text{Mass}} \right. \\
 & + \rho_p \left(\underbrace{\mathbf{u} \cdot \nabla p + M^2 \tau : \nabla \mathbf{u}}_{\text{Momentum}} - \underbrace{\nabla \cdot (\rho h \mathbf{u}) + \nabla \cdot \mathbf{q}_e}_{\text{Total Energy}} \right) \\
 & \left. + \sum_{i=1}^{N-1} \left(\rho_p h_{Y_i} - \rho_{Y_i} \rho_T \frac{T}{\rho^2} \right) \left(\underbrace{\nabla \cdot (\rho Y_i \mathbf{u}) - \nabla \cdot \mathbf{q}_i - \dot{\omega}_i}_{\text{Species}} \right) \right\}
 \end{aligned}$$

where

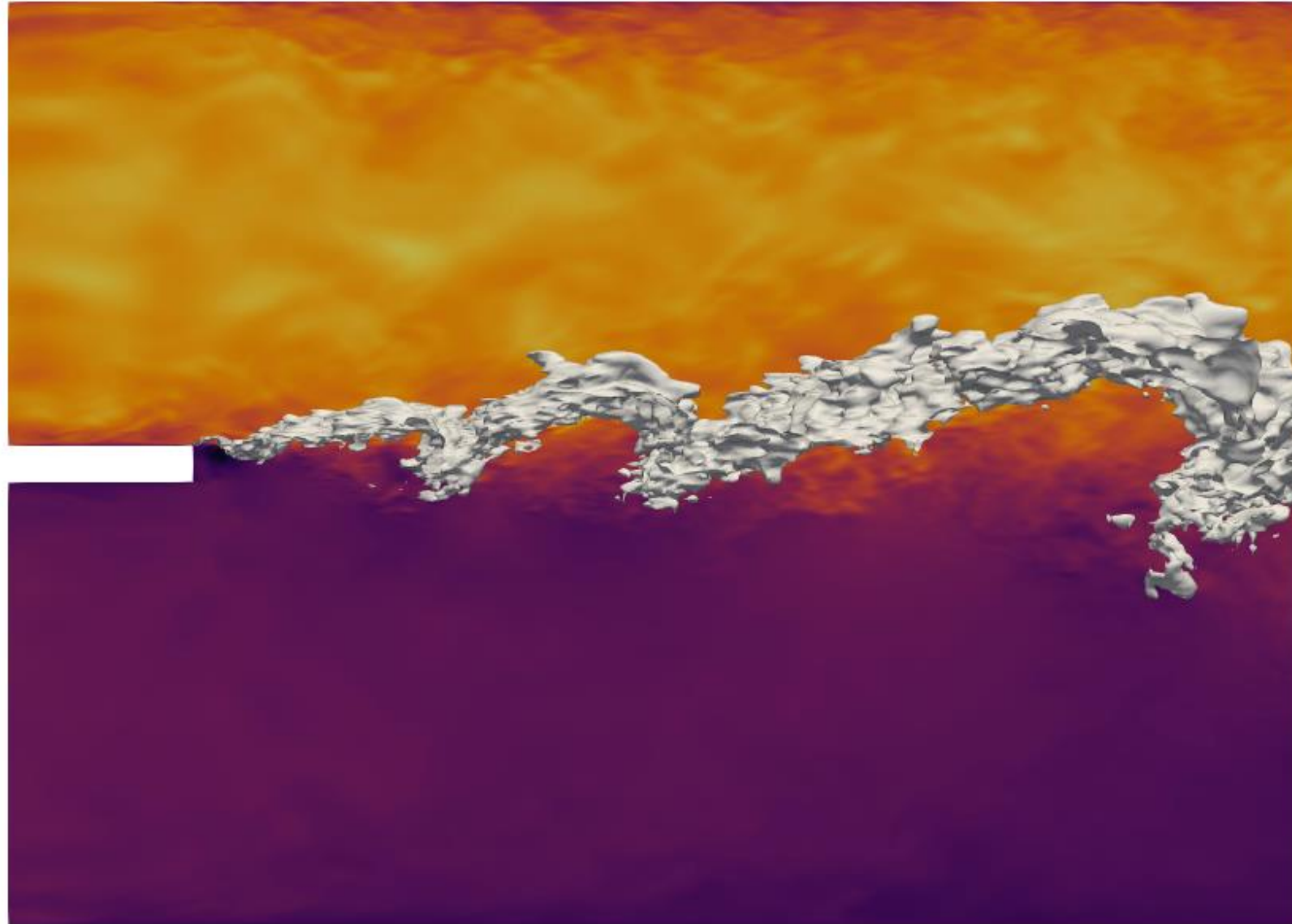
$$\frac{c^2}{\rho C_p} = \frac{1}{\rho_p \rho C_p + \rho_T (1 - \rho h_p)} = \frac{1}{\rho} \left[\frac{1}{\alpha \rho C_p - \beta (1 - \rho h_p)} \right] = \frac{1}{\rho} \left[\frac{1}{\alpha \rho C_p - \beta^2 T} \right]$$

Variation of isothermal compressibility across three-dimensional mixing layer

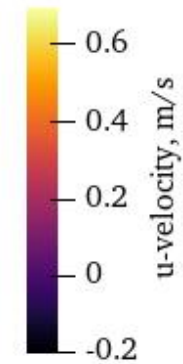


$$\alpha = \frac{1}{\rho} \left(\frac{\partial \rho}{\partial p} \right)_{T, Y_1, \dots, Y_N}$$

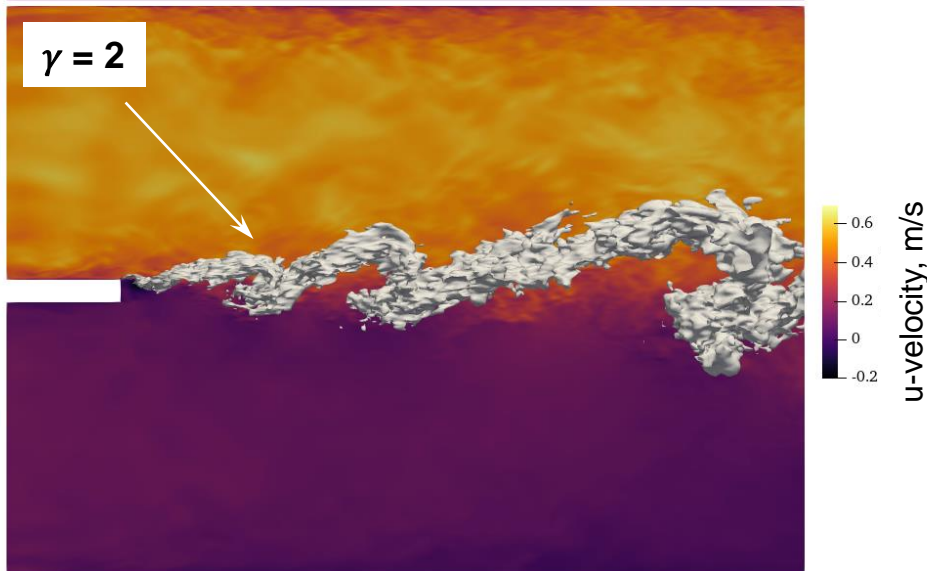
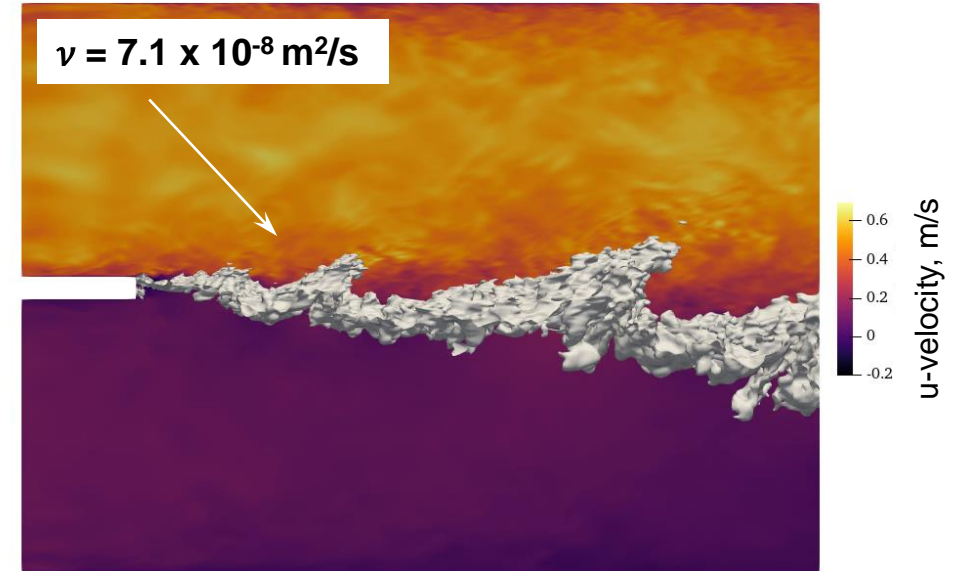
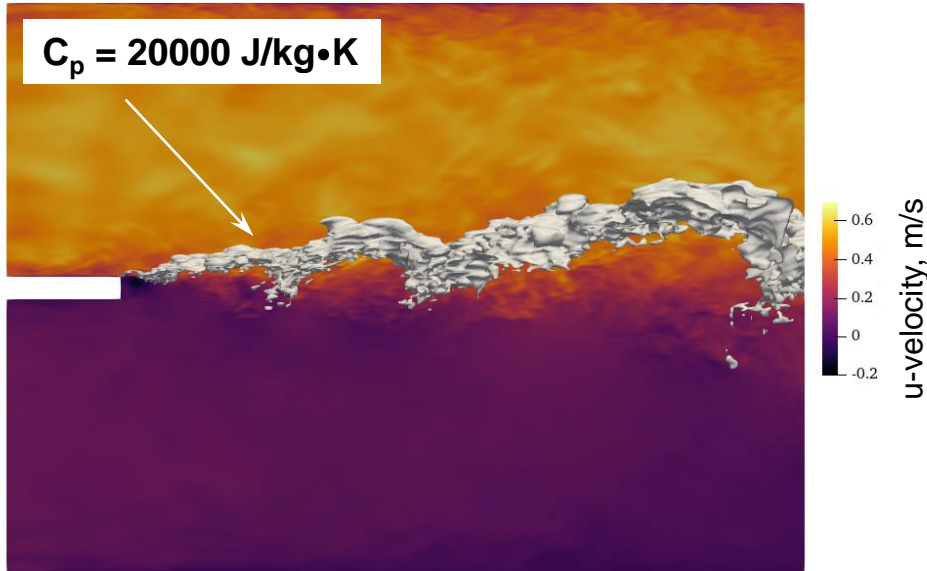
Isosurface showing threshold where the coefficient of thermal expansion is 0.15



$$\beta = -\frac{1}{\rho} \left(\frac{\partial \rho}{\partial T} \right)_{p, Y_1, \dots, Y_N}$$



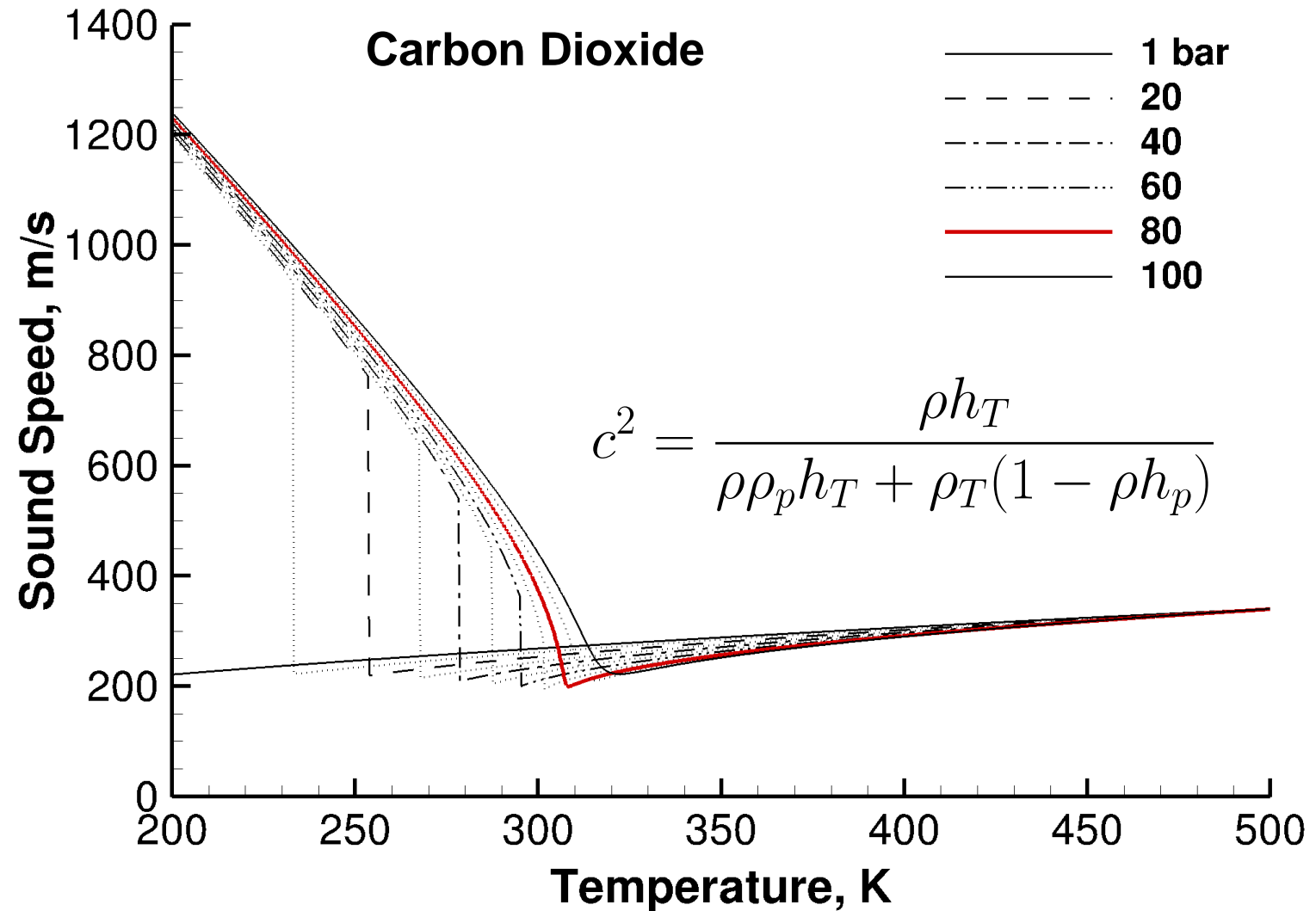
Ratio of $c^2/\rho C_p$ also modulates observables in highly nonlinear manner



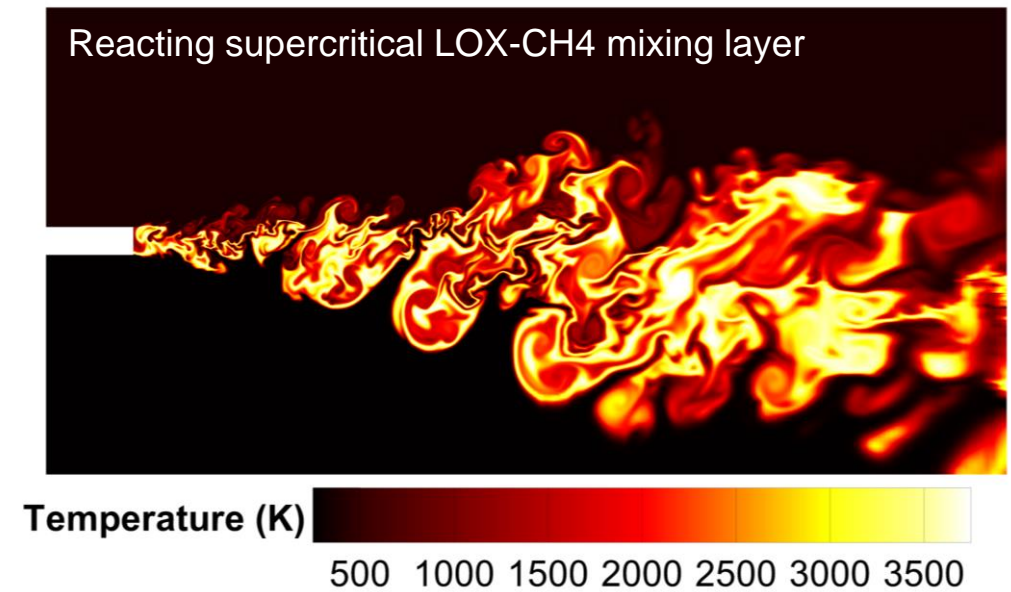
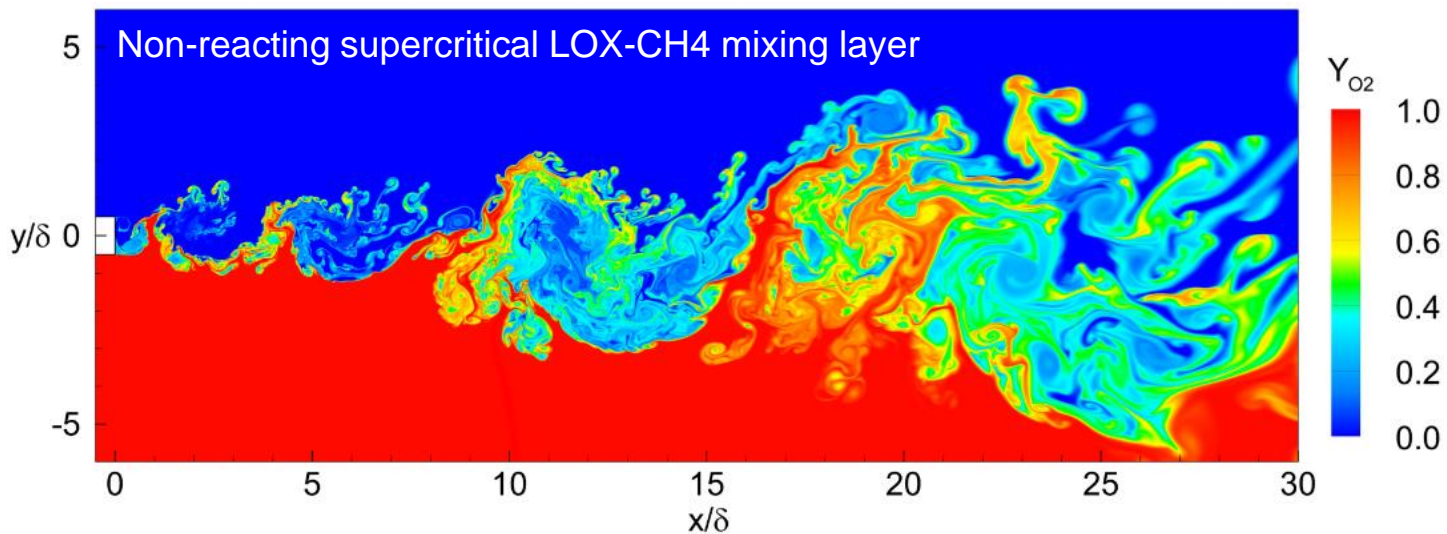
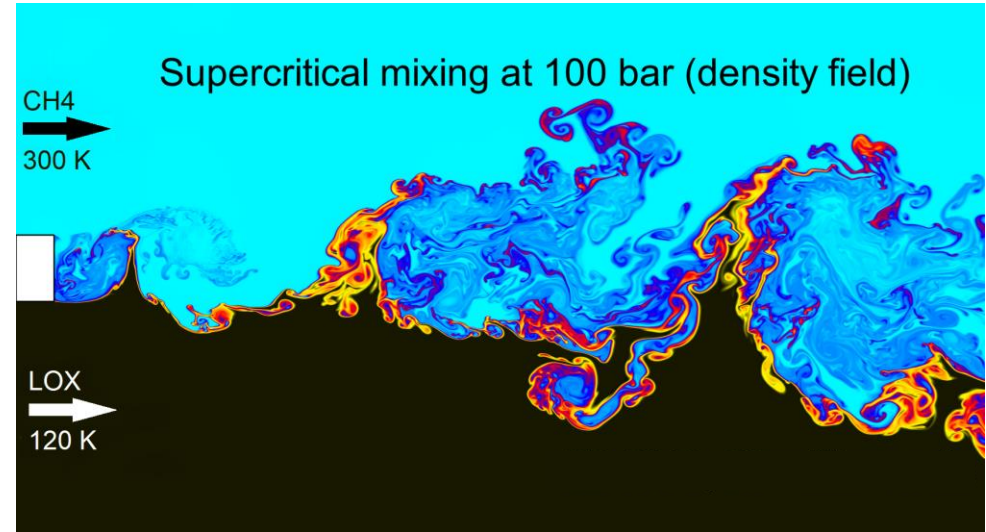
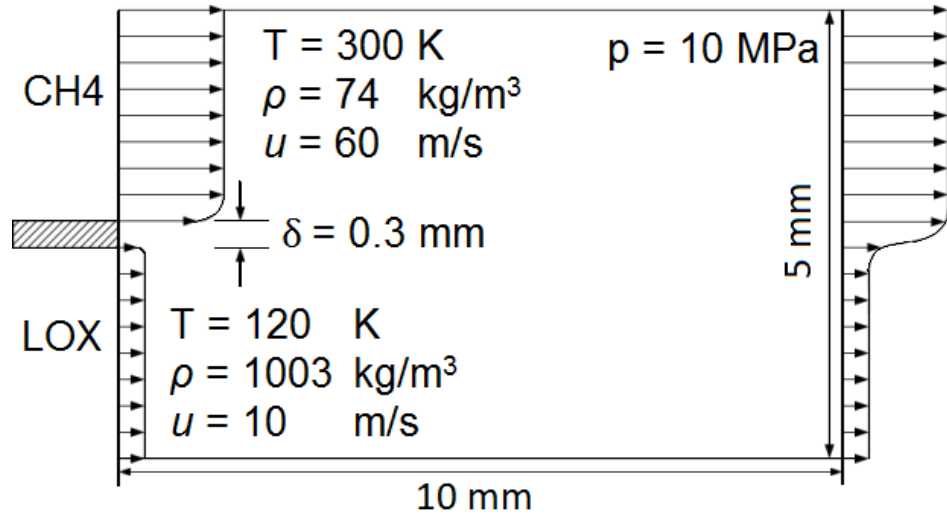
Transport properties exhibit similar behavior

“Interim” summary and observations ...

- Thermodynamic nonidealities and transport anomalies impose additional nonlinearities that modulate both broadband turbulence characteristics and observables (e.g., multiscale mixing)
- Alters both the instantaneous and filtered equations for LES identically*
 - i.e., they premultiply convective/diffusive operators and source terms in both sets of equations and thus modulate these terms in the same way
 - *Additional focus needs to be placed on filtering nonlinear EOS and related properties (in progress)
- Chemical source term Jacobians and related eigenvalues also involve ρ_p and ρ_T
 - i.e., compressibility and thermodynamic nonidealities also affect finite-rate chemical kinetics and related stiffness in chemistry
- Nonequilibrium turbulence, baroclinic torque, etc., also significant factors
- Analysis of results is ongoing



Reacting flow studies ...



Many additional terms arise as consequence of filtering compressible multicomponent conservation equations

- Filtered Mass:

$$\frac{\partial \bar{\rho}}{\partial t} + \nabla \cdot (\bar{\rho} \tilde{\mathbf{u}}) = 0. \quad (1)$$

- Filtered Momentum:

$$\frac{\partial}{\partial t}(\bar{\rho} \tilde{\mathbf{u}}) + \nabla \cdot \left(\bar{\rho} \tilde{\mathbf{u}} \otimes \tilde{\mathbf{u}} + \frac{\bar{p}}{M^2} \mathbf{I} \right) = \nabla \cdot \bar{\boldsymbol{\tau}} - \nabla \cdot \mathbf{T}, \quad (2)$$

where

$$\bar{\boldsymbol{\tau}} = \overline{\frac{\mu}{Re} \left[-\frac{2}{3}(\nabla \cdot \mathbf{u})\mathbf{I} + (\nabla \mathbf{u} + \nabla \mathbf{u}^T) \right]}.$$

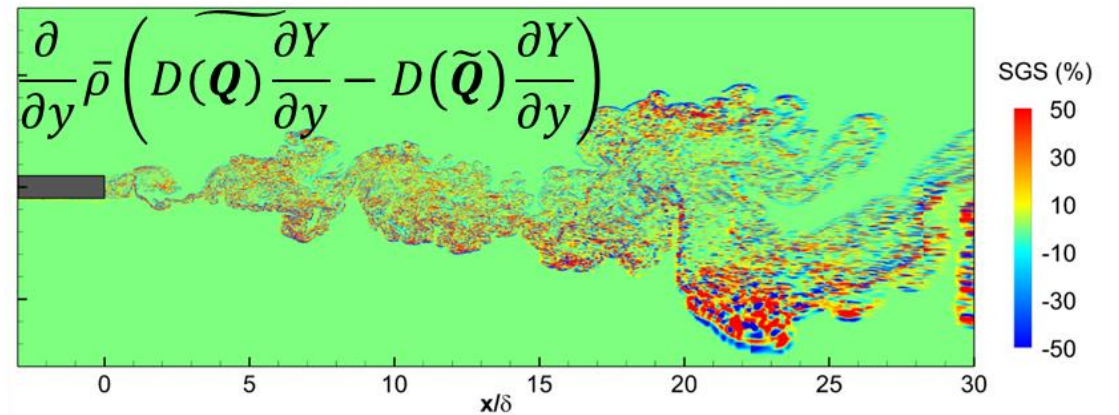
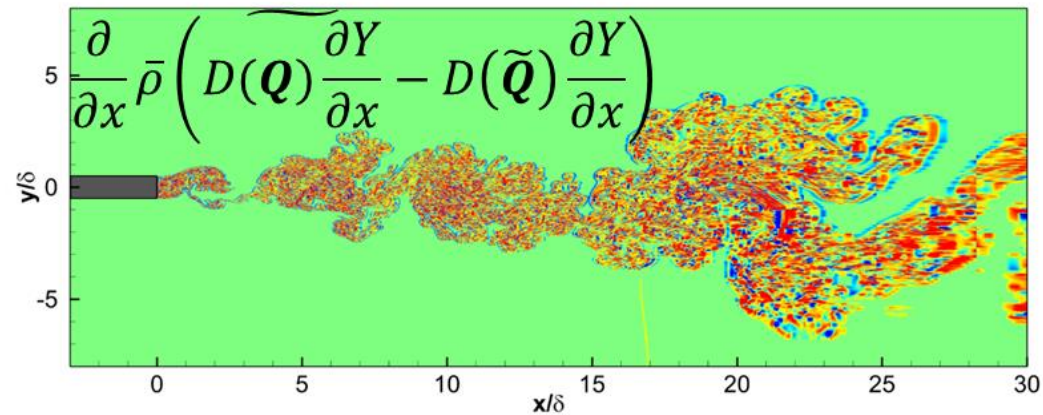
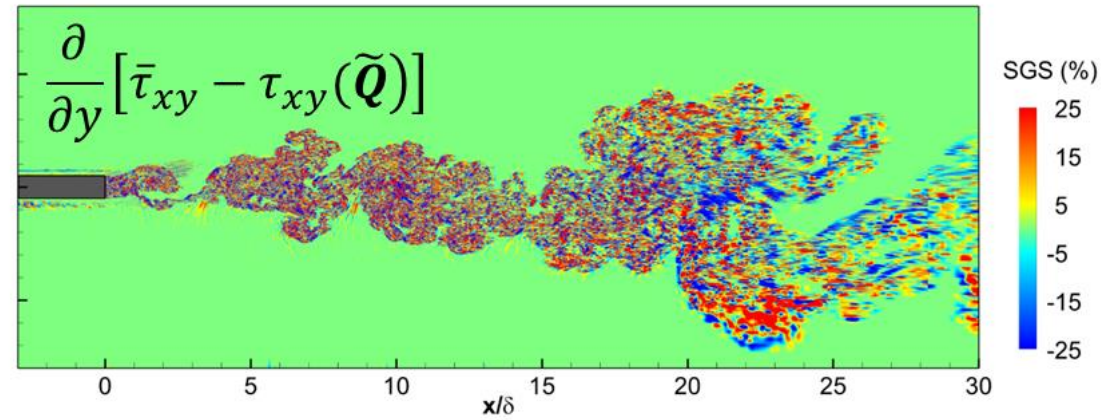
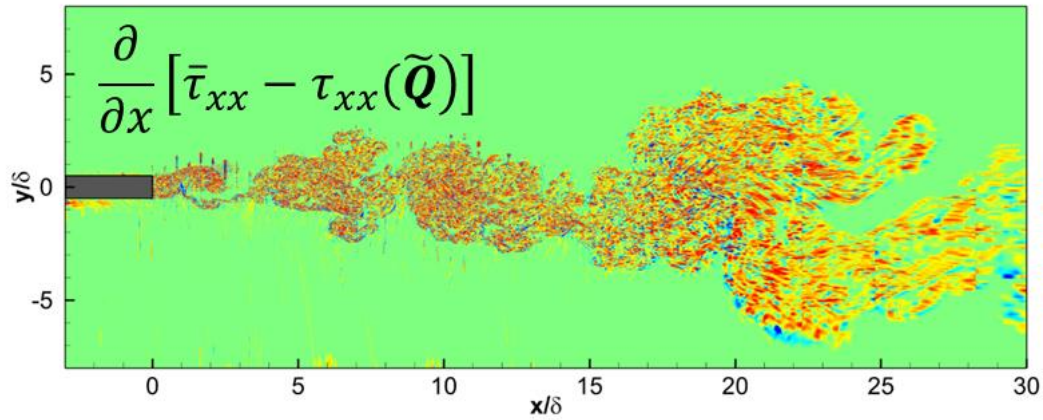
- Filtered Species:

$$\frac{\partial}{\partial t}(\bar{\rho} \tilde{Y}_i) + \nabla \cdot (\bar{\rho} \tilde{Y}_i \tilde{\mathbf{u}}) = \nabla \cdot \bar{\mathbf{q}}_i - \nabla \cdot \bar{\mathbf{S}}_i + \bar{\dot{\omega}}_i \quad i = 1, \dots, N - 1, \quad (3)$$

where

$$\bar{\mathbf{q}}_i = \overline{\frac{\mu}{Sc_i Re} \nabla Y_i}.$$

e.g., Variances of viscous stress tensor and diffusion fluxes can be significant depending on filter width



Filter size 10x larger relative to DNS ($\Delta_{LES}/\Delta_{DNS} = 10$)

Filtered total energy equation

- Filtered Total Energy:

$$\begin{aligned}
 \frac{\partial}{\partial t}(\bar{\rho}\tilde{e}_t) + \nabla \cdot [(\bar{\rho}\tilde{e}_t + \bar{p})\tilde{\mathbf{u}}] &= \nabla \cdot (\bar{\mathbf{q}}_e + M^2(\bar{\boldsymbol{\tau}} \cdot \tilde{\mathbf{u}})) \\
 &- \nabla \cdot (\mathbf{Q} + M^2(\mathbf{T} \cdot \tilde{\mathbf{u}})) \\
 &- \nabla \cdot \left[\frac{M^2}{2} \text{tr}(\mathbf{T}\tilde{\mathbf{u}}'') \right] + \nabla \cdot (M^2(\overline{\boldsymbol{\tau} \cdot \mathbf{u}}'')) + \bar{\dot{Q}}_e,
 \end{aligned} \tag{4}$$

where

$$\begin{aligned}
 \tilde{e}_t &= \tilde{e} + \frac{M^2}{2} \tilde{\mathbf{u}} \cdot \tilde{\mathbf{u}} + \frac{M^2 \text{tr}(\mathbf{T})}{2\bar{\rho}}, \\
 \tilde{e} &= \sum_{i=1}^N \tilde{h}_i \tilde{Y}_i - \frac{\bar{p}}{\bar{\rho}} + \sum_{i=1}^N \left[(\widetilde{\tilde{h}_i \tilde{Y}_i} - \tilde{h}_i \tilde{Y}_i) + (\widetilde{\tilde{h}_i Y_i''} + \widetilde{h_i'' \tilde{Y}_i}) + \widetilde{h_i'' Y_i''} \right], \\
 \bar{\dot{Q}}_e &= - \sum_{i=1}^N \bar{\dot{\omega}}_i h_{f_i}^\circ, \text{ and } \bar{\mathbf{q}}_e = \overline{\frac{\mu C_p}{Pr Re} \nabla T} + \sum_{i=1}^N \overline{h_i \mathbf{q}_i}.
 \end{aligned}$$

Consistent modeling of SFS variances/covariances rare, enthalpy/EOS must also be filtered and require closures

- Turbulent Momentum, Energy, and Species Fluxes:

$$\mathbf{T} = \bar{\rho}(\widetilde{\tilde{\mathbf{u}}} \otimes \tilde{\mathbf{u}} - \tilde{\mathbf{u}} \otimes \tilde{\mathbf{u}}) + \bar{\rho}(\widetilde{\tilde{\mathbf{u}}} \otimes \mathbf{u}'' + \widetilde{\mathbf{u}''} \otimes \tilde{\mathbf{u}}) + \bar{\rho}\widetilde{\mathbf{u}'' \otimes \mathbf{u}''}$$

$$\mathbf{Q} = \bar{\rho}(\widetilde{\tilde{h}\tilde{\mathbf{u}}} - \tilde{h}\tilde{\mathbf{u}}) + \bar{\rho}(\widetilde{\tilde{h}\mathbf{u}''} + \widetilde{h''\tilde{\mathbf{u}}}) + \bar{\rho}\widetilde{h''\mathbf{u}''}$$

$$\mathbf{S}_i = \bar{\rho}(\widetilde{\tilde{Y}_i\tilde{\mathbf{u}}} - \tilde{Y}_i\tilde{\mathbf{u}}) + \bar{\rho}(\widetilde{\tilde{Y}_i\mathbf{u}''} + \widetilde{Y_i''\tilde{\mathbf{u}}}) + \bar{\rho}\widetilde{Y_i''\mathbf{u}''}$$

- Enthalpy:

$$\bar{\rho}\tilde{e} + \bar{p} = \bar{\rho} \sum_{i=1}^N \tilde{h}_i \tilde{Y}_i + \bar{\rho} \sum_{i=1}^N \left[(\widetilde{\tilde{h}_i \tilde{Y}_i} - \tilde{h}_i \tilde{Y}_i) + (\widetilde{\tilde{h}_i \mathbf{u}''} + \widetilde{h_i'' \tilde{\mathbf{u}}}) + \widetilde{h_i'' \mathbf{u}''} \right]$$

- Equation of State:

$$\bar{p} = \bar{\rho} R_u \sum_{i=1}^N \left(\frac{\tilde{T} \tilde{Y}_i}{W_i} + \frac{(\widetilde{\tilde{T} \tilde{Y}_i} - \tilde{T} \tilde{Y}_i) + (\widetilde{\tilde{T} \mathbf{u}''} + \widetilde{T'' \tilde{\mathbf{u}}}) + \widetilde{T'' \mathbf{u}''}}{W_i} \right)$$

- Filtered Viscous Stress Tensor, and Filtered Energy and Mass Diffusion Fluxes

“Mixed” Dynamic Smagorinsky (DMM) model shown below is consistent, DSM is not since it neglects terms

- Eddy Viscosity:

$$\mu_t = \bar{\rho} C_R \Delta^2 \Pi_{\tilde{\mathbf{S}}}^{\frac{1}{2}} \quad \Pi_{\tilde{\mathbf{S}}} = \tilde{\mathbf{S}} : \tilde{\mathbf{S}} \quad \tilde{\mathbf{S}} = \frac{1}{2} (\nabla \tilde{\mathbf{u}} + \nabla \tilde{\mathbf{u}}^T)$$

- Stress Tensor:

$$\vec{\mathcal{T}} = (\bar{\boldsymbol{\tau}} - \mathbf{T}) = (\mu_t + \mu) \frac{1}{Re} \left[-\frac{2}{3} (\nabla \cdot \tilde{\mathbf{u}}) \mathbf{I} + (\nabla \tilde{\mathbf{u}} + \nabla \tilde{\mathbf{u}}^T) \right] - \bar{\rho} \left(\widetilde{\tilde{\mathbf{u}} \otimes \tilde{\mathbf{u}}} - \tilde{\mathbf{u}} \otimes \tilde{\mathbf{u}} \right) - \frac{1}{3} \bar{\rho} q_{\text{sfs}}^2 \mathbf{I}$$

- Energy Flux:

$$\vec{\mathcal{Q}}_e = (\bar{\mathbf{q}}_e - \mathbf{Q}) = \left(\frac{\mu_t}{Pr_t} + \frac{\mu}{Pr} \right) \frac{1}{Re} \nabla \tilde{h} + \sum_{i=1}^N \tilde{h}_i \vec{\mathcal{S}}_i - \bar{\rho} \left(\widetilde{\tilde{h} \tilde{\mathbf{u}}} - \tilde{h} \tilde{\mathbf{u}} \right)$$

- Mass Flux:

$$\vec{\mathcal{S}}_i = (\bar{\mathbf{q}}_i - \mathbf{S}_i) = \left(\frac{\mu_t}{Sc_{t_i}} + \frac{\mu}{Sc_i} \right) \frac{1}{Re} \nabla \tilde{Y}_i - \bar{\rho} \left(\widetilde{\tilde{Y}_i \tilde{\mathbf{u}}} - \tilde{Y}_i \tilde{\mathbf{u}} \right)$$

Coefficients C_R , Pr_t , and Sc_{t_i} evaluated dynamically as functions of space and time

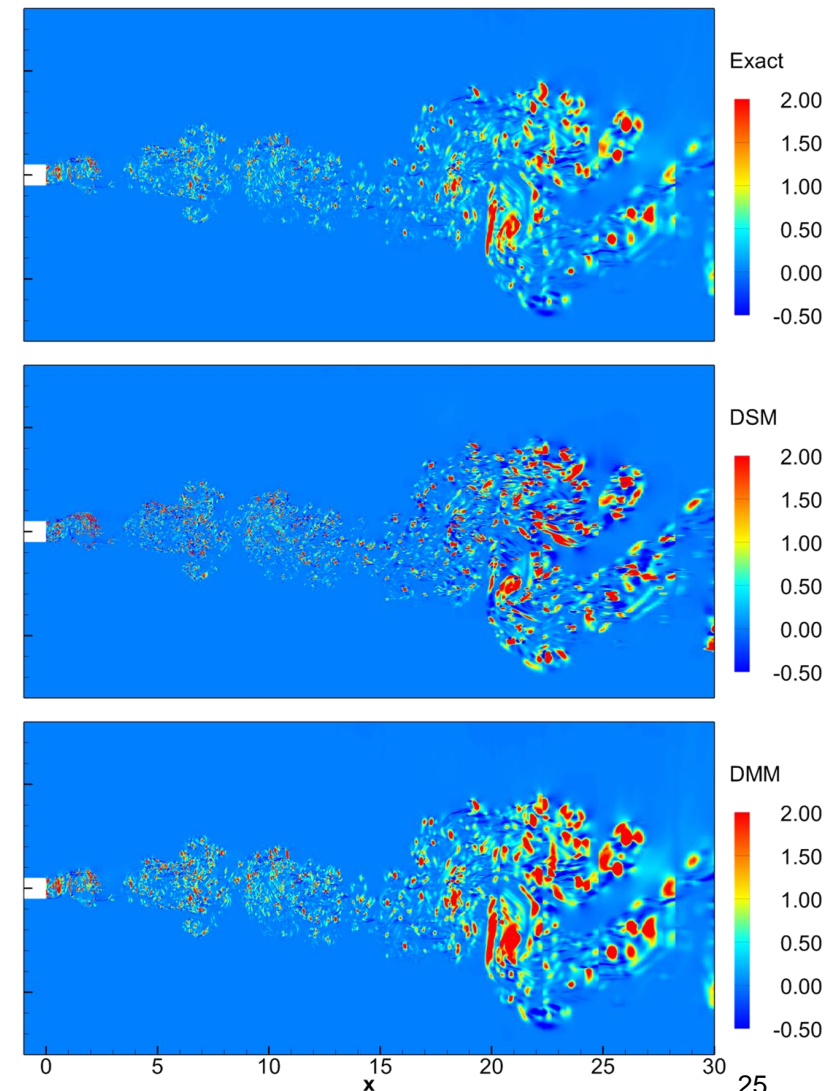
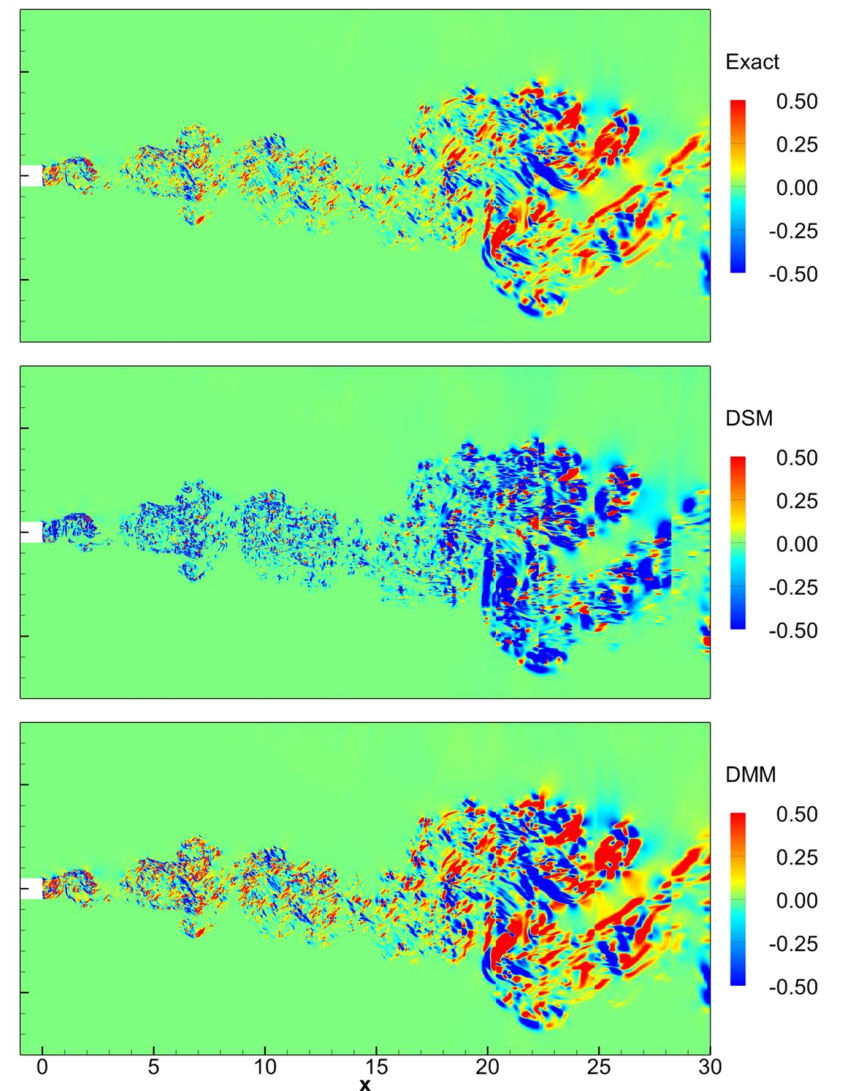
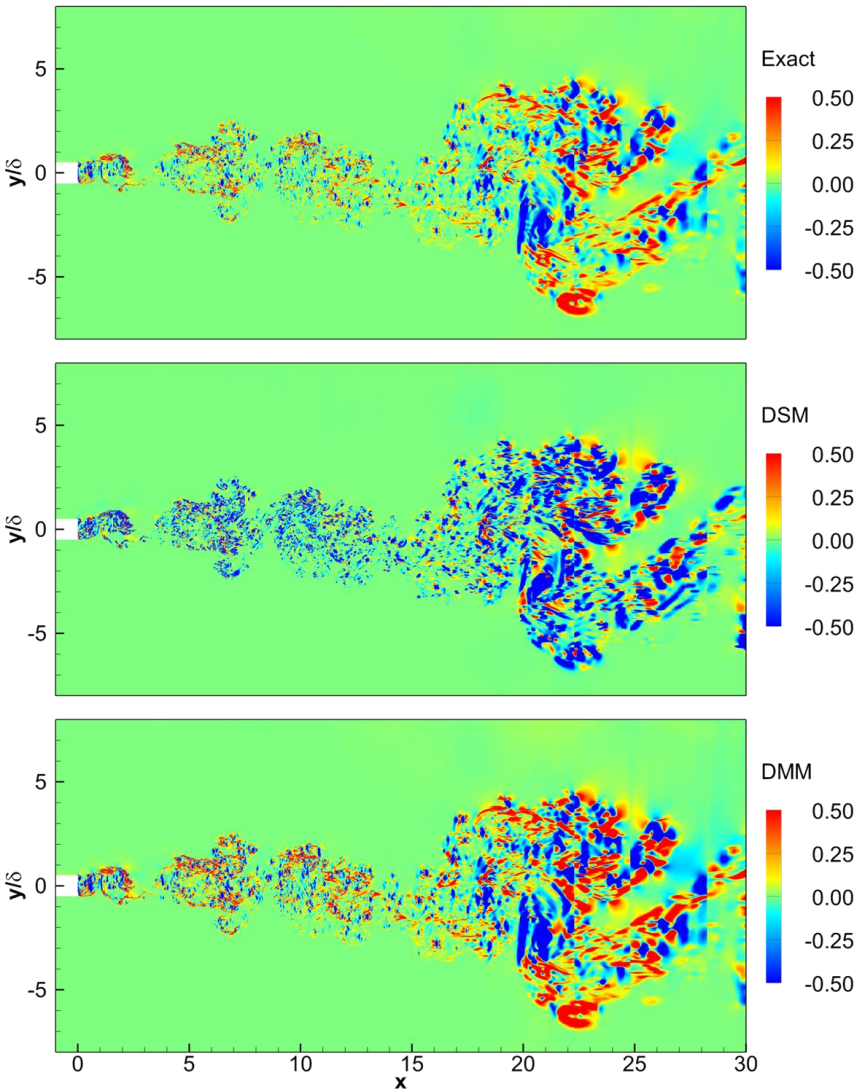
A priori assessment of Dynamic Smagorinsky Model versus Dynamic Mixed Model

$(\Delta_{LES}/\Delta_{DNS} = 5)$

$$\widetilde{u\tilde{u}} - \tilde{u}\tilde{u}$$

$$\widetilde{u\tilde{v}} - \tilde{u}\tilde{v}$$

$$\widetilde{v\tilde{v}} - \tilde{v}\tilde{v}$$



A priori assessment of Dynamic Smagorinsky (DSM) versus Mixed Dynamic Smagorinsky (DMM)

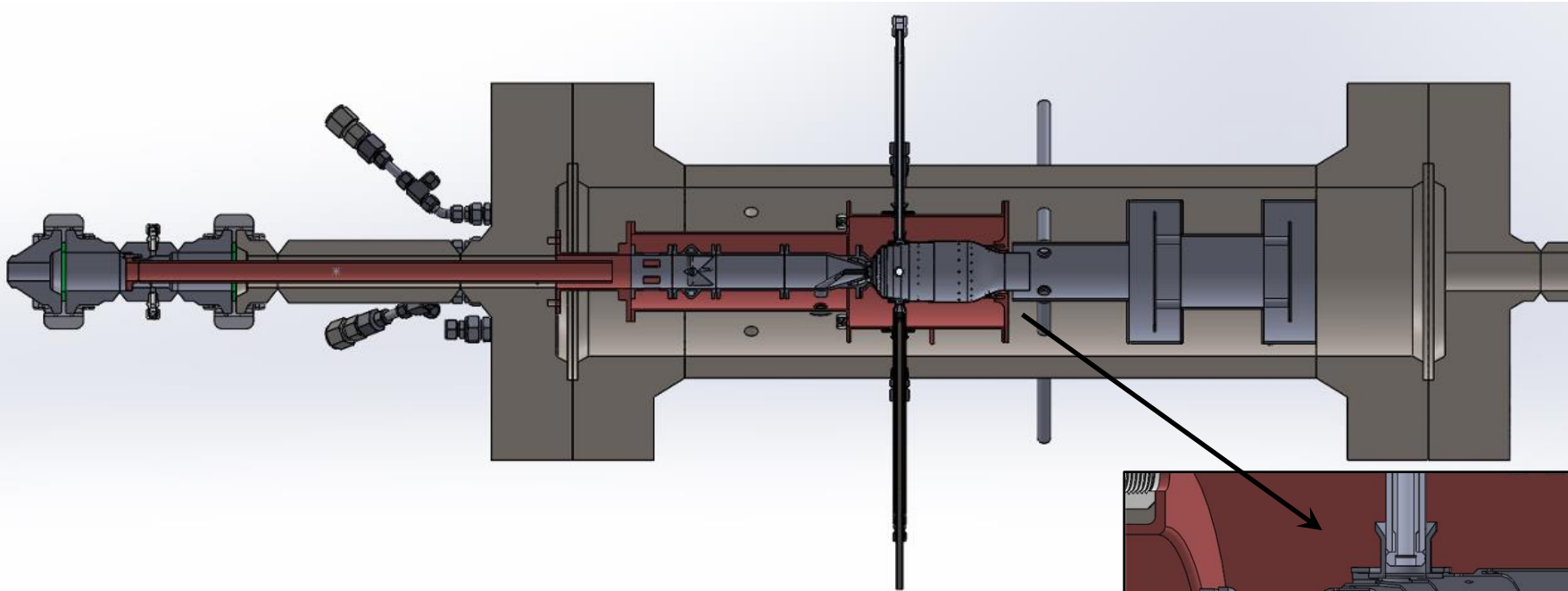
Covariance	Dynamic Smagorinsky	Mixed Dynamic Smagorinsky
$(\widetilde{uu})_{\text{sfs}}$	65.7 %	82.8 %
$(\widetilde{uv})_{\text{sfs}}$	84.2 %	89.8 %
$(\widetilde{vv})_{\text{sfs}}$	53.0 %	90.7 %
$(\widetilde{uT})_{\text{sfs}}$	69.8 %	92.2 %
$(\widetilde{vT})_{\text{sfs}}$	74.8 %	91.0 %
$(\widetilde{uY})_{\text{sfs}}$	68.0 %	74.6 %
$(\widetilde{vY})_{\text{sfs}}$	61.6 %	92.7 %

Filter size 5x larger relative to DNS ($\Delta = 5$).

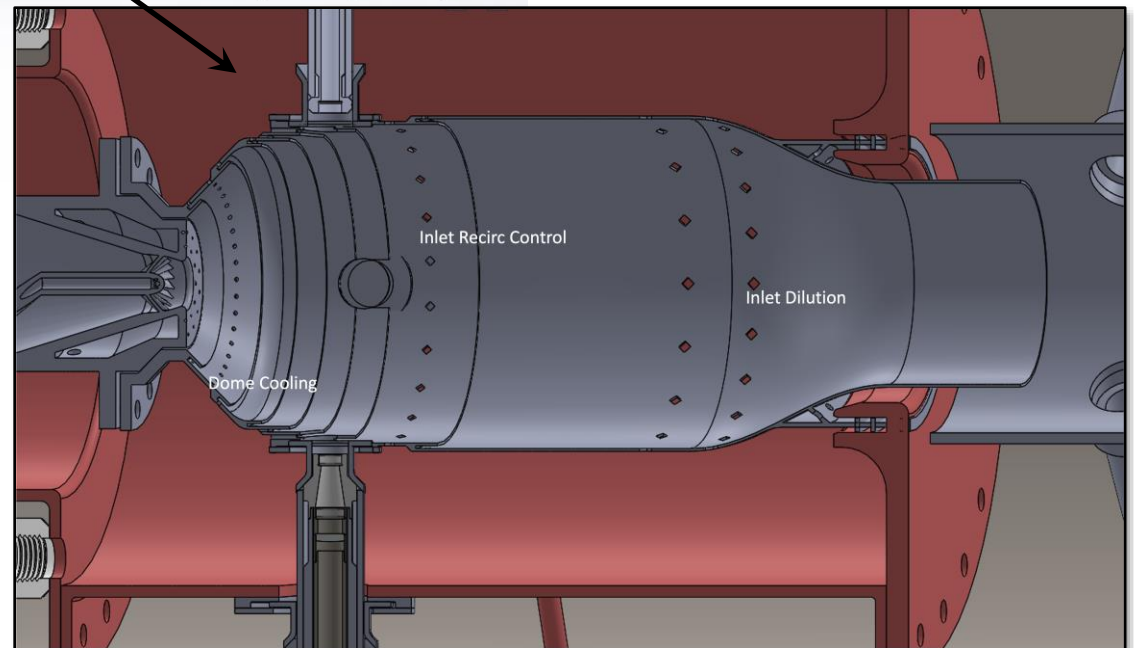
A priori assessment of Dynamic Smagorinsky (DSM) versus Mixed Dynamic Smagorinsky (DMM)

Covariance		Dynamic Smagorinsky	Mixed Dynamic Smagorinsky
$(\widetilde{uv})_{\text{sfs}}$	$\Delta = 5$	84.2 %	89.8 %
	$\Delta = 10$	17.2 %	60.9 %
$(\widetilde{uT})_{\text{sfs}}$	$\Delta = 5$	69.8 %	92.2 %
	$\Delta = 10$	9.3 %	33.5 %
$(\widetilde{vY})_{\text{sfs}}$	$\Delta = 5$	61.6 %	92.7 %
	$\Delta = 10$	18.8 %	58.9 %

Concurrent work ... collaborations initiated with SwRI on simulations of direct fired supercritical oxy-combustion



- High-resolution first-principles LES that identically matches geometry and operating conditions combined with close collaborations with SwRI CFD group
- Analysis of sub-model accuracy and performance in a complex geometric environment; e.g.,
 - Turbulent velocity and multiscale mixing
 - Turbulent mixed-mode combustion
 - Finite-rate chemical kinetics
 - Best practices for model implementation

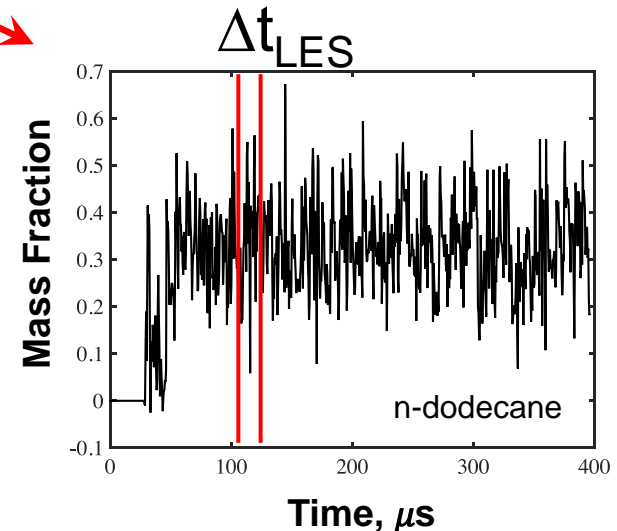


Concurrent work ... collaborations initiated with SwRI on simulations of direct fired supercritical oxy-combustion

$$\bar{\omega}_i(\mathbf{x}, t) = \int_t^{t+\Delta t} \left\{ \iiint_{V(\tau)} \mathcal{G}(\mathbf{y} - \mathbf{x}, \tau - t; \delta \mathbf{y}, \delta \tau) \dot{\omega}_i(\phi_1, \phi_2, \dots; \mathbf{y}, \tau) dV \right\} d\tau$$

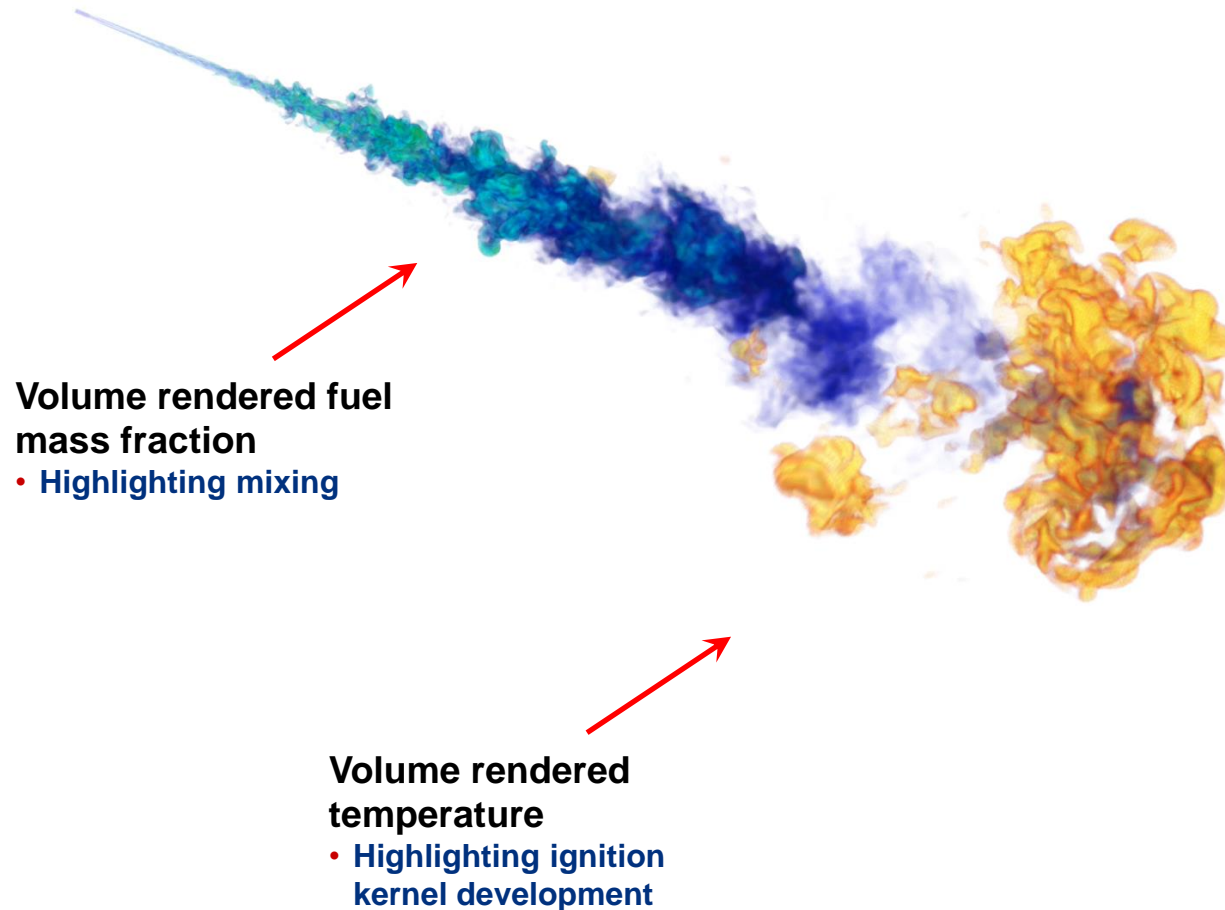
$$\phi_i(\mathbf{x}, t) = \tilde{\phi}_i(\mathbf{x}, t) + \phi_i''(\mathbf{x}, t)$$

- Currently investigating the merits of a new combustion closure based on space-time filtering
- Hypothesis ... space-time filtering can be used to close the filtered chemical source terms directly
 - Apply approximate deconvolution model with assumed scalar spectrum to calculate subfilter variance/covariance matrix
 - Variance/covariance matrix used as input to generate correlated scalar fluctuations on subfilter scales in time
 - Use modeled instantaneous signal to evaluate filtered chemical source terms directly
- Benefits ... **1)** conceptually regime independent, **2)** minimizes assumptions required for closure, **3)** approaches correct behavior in limit of DNS (i.e., facilitates hybrid-DNS/LES approach)



e.g., Modeled instantaneous fluctuations of fuel-air mixture on centerline at 100 diameters downstream of injection

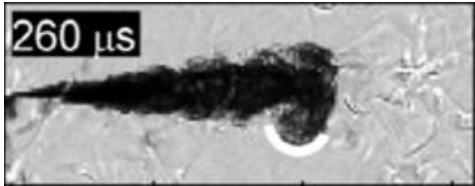
e.g., Modeled instantaneous fluctuations facilitate formation of ignition kernels on subfilter time scales



Major goal is to tightly couple simulations to complex companion experiments (i.e., SwRI rig)

First kernel, diameter $\approx 500 \mu\text{m}$
(too small to be optically detected)
Location: tip of the jet, off-axis

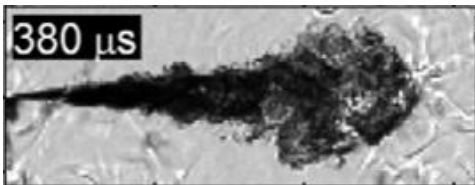
Independent kernels appear,
diameter $\approx 500 \mu\text{m}$ to 2mm (still
very small for optical detection)
Location: tip of the jet, off-axis



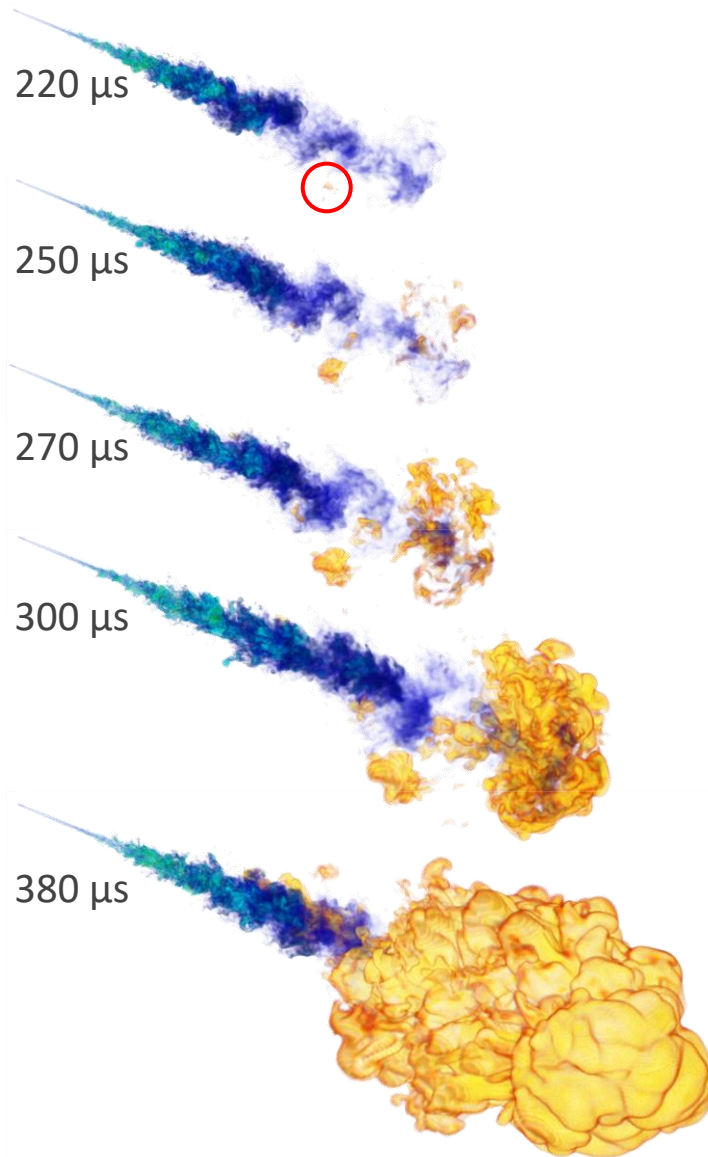
Many small kernels present in the "jet edge" region, what is the impact on Schlieren?

Single flame structure with upstream independent kernels, flame expands through dilatation and autoignition

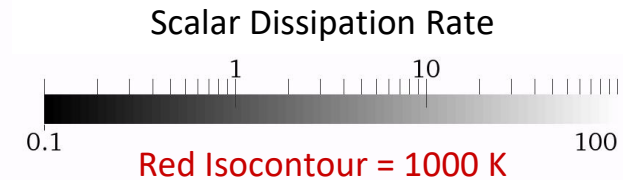
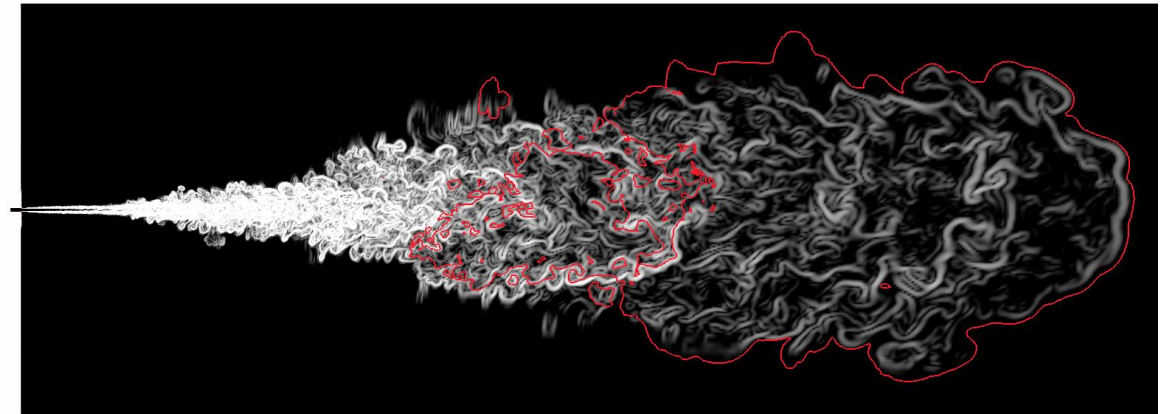
Main flame region at the jet extremity, autoignition locations observed ahead of main front



Schlieren images by Skeen *et al.*, PCI, 2015



e.g., Enable unique analysis of processes that can't be measured at conditions that match experiments



- 3D high-repetition flow-flame interactions, dynamics of scalar-dissipation and its effects on chemical kinetics
- Converting simulation data to modeled signals produced via laser diagnostics for enhanced analysis in complex environments

Summary

- **Details related to fundamental physics and modeling for LES for compressible flows and supercritical fluids**
 - **Numerous additional terms appear in the filtered conservation equations as a result of the filtering process**
 - Compressibility effects and nonequilibrium turbulence apply to all compressible flows
 - Scalar-scalar variance/covariances associated with filtered total energy equation, EOS, enthalpy
 - Viscous stress tensor, energy diffusion, and mass diffusion fluxes
 - **Terms need to be treated through combination of consistency, modeling, and quantified resolution requirements**
 - Demonstrated process for establishing resolution requirements related to scalar mixing
 - Mixed Dynamic Smagorinsky (DMM) model is consistent and thus more accurate as function of resolution
 - Dynamic Smagorinsky model is not consistent since it neglects terms
 - **Future work will incorporate treatment of scalar-scalar variances and the filtered mass, momentum, energy diffusion fluxes (e.g., what can we control via resolution constraints, what needs to be modeled)**
- **Anomalies associated with multiscale mixing and combustion in context of direct fired supercritical oxy-combustion LRE's at supercritical pressures**
 - **Thermodynamic nonidealities and transport anomalies impose additional nonlinearities that modulate both broadband turbulence characteristics and observables (e.g., multiscale mixing, pressure, temperature)**
 - Demonstrated how nonlinearities in EOS, thermodynamics, transport can modulate local flow characteristics
 - Compressibility and thermodynamic nonlinearities also affect finite-rate chemical kinetics
 - **Future work will focus on modeling filtered EOS and related thermodynamic and transport properties as well as nonequilibrium turbulence, baroclinic torque, etc., which are significant factors that require further investigation**